Optimal Joint Target Detection and Parameter Estimation by MIMO Radar

Ali Tajer, *Student Member, IEEE*, Guido H. Jajamovich, *Student Member, IEEE*, Xiaodong Wang, *Fellow, IEEE*, and George V. Moustakides, *Senior Member, IEEE*

Abstract—We consider multiple-input multiple-output (MIMO) radar systems with widely spaced antennas. Such antenna configuration facilitates capturing the inherent diversity gain due to independent signal dispersion by the target scatterers. We consider a new MIMO radar framework for detecting a target that lies in an *unknown* location. This is in contrast with conventional MIMO radars which break the space into small cells and aim at detecting the presence of a target in a specified cell. We treat this problem through offering a novel composite hypothesis testing framework for target detection when 1) one or more parameters of the target are unknown and we are interested in estimating them, and 2) only a *finite* number of observations are available. The test offered optimizes a metric which accounts for both detection and estimation accuracies. In this paper, as the parameter of interest we focus on the vector of time-delays that the waveforms undergo from being emitted by the transmit antennas until being observed by the receive antennas. The analytical and empirical results establish that for the proposed joint target detection and time-delay estimation framework, MIMO radars exhibit significant gains over phased-array radars for extended targets which consist of multiple independent scatterers. For point targets modeled as single scatterers, however, the detection/estimation accuracies of MIMO and phased-array radars for this specific setup (joint target detection and time-delay estimation) are comparable.

Index Terms—Diversity gain, finite-sample, generalized likelihood ratio test (GLRT), joint estimation/detection.

I. INTRODUCTION

INSPIRED by the diversity gains yielded by multiple-input multiple-output (MIMO) communication systems for alleviating wireless fading impediments, the concept of MIMO radar systems has been first introduced in [1] and further developed in [2]–[8]. The underlying idea of MIMO radar for offering diversity gains is to illuminate uncorrelated waveforms at the target such that their corresponding reflections remain uncorrelated and hence offer independent observations of the target. It has been demonstrated that such diversities in observing the target bring about performance improvement by enhancing the accuracy in detecting the target and estimating its associated parameters, e.g., range, speed, and direction.

MIMO radar systems can be exploited for capturing radar cross section (RCS) diversity via deploying widely separated antennas [4], or for establishing more degrees of freedom by configuring co-located antennas [9]. While the former configuration improves detection and estimation qualities and supports high-resolution target localization [5], the latter one enhances the power of probing in the vicinity of target location [6], [7], [10].

In this paper, we consider a widely spaced antenna configuration and treat two problems. First, we analyze the problem of target detection when some radar parameters are unknown and needed to be estimated. We offer a framework for joint target detection and parameter estimation (with optimality properties provided in Section III) when the receive antennas can acquire only a *finite* number of observations. While the proposed framework can be exploited for detecting the target in conjunction with estimating any parameter of interest, we consider the problem of detecting a target that lies in an unknown location. In our formulation, the uncertainty about the target location is accounted for through the time-delays that the transmitted waveforms undergo before reaching the receive antennas. We formulate this problem as a composite hypothesis test which is shown to be solved optimally via the widely known generalized likelihood ratio test (GLRT). Note that the existing optimality results of the GLRT hold only asymptotically for an *infinite* number of observations under certain assumptions [11, Sec. 5.6].

As the second problem, we analyze the diversity gain of the proposed detector, which is defined as the decay rate of the mis-detection probability with the increasing signal-to-noise ratio (SNR) for a fixed false alarm probability [4]. We analytically quantify the diversity gain as a function of the number of transmit and receive antennas. This notion of diversity gain for MIMO radars has been first examined for MIMO radars in [3] and [4] for the MIMO radar model introduced in [3], which considers detecting the presence of a target at a given location. It is noteworthy that another notion of diversity gain defined as the detector's divergence in high SNR regimes has also been analyzed in [3].

We treat the two aforementioned problems for two target models: point targets which are modeled as single scatterers [4], [5]; and extended targets, which are comprised of many isotropic and independent scatterers. The summary of the contributions and results of this work is as follows.

We propose an optimality measure which is shaped by target detection performance, parameter estimation accuracy and false alarm probability. The corresponding optimal composite hypothesis test that satisfies some optimality criteria is introduced

and deployed for detecting a target in an unknown location. Next, for an $N_t \times N_r$ MIMO radar system we characterize the maximum likelihood (ML) estimate of the time-delay vector which consists of $N_t N_r$ components corresponding to different pairs of transmit–receive antennas. The optimal detector corresponding to such ML estimate is also derived. This detector differs from the existing ones in the literature in the sense that it aims at detecting a target in an unknown location, whereas the existing MIMO radar detectors break the space into small cells and detect the presence of the target in a specific cell. Finally, we demonstrate that for the proposed detector, in an $N_t \times N_r$ MIMO radar system with widely spaced antennas and with an upper-limit constraint on the false alarm probability, the mis-detection probability decays as $\mathrm{SNR}^{-N_t N_r}$ for extended targets and decays as SNR^{-1} for point targets. Such mis-detection probability in phased-array radars for both extended and point targets is shown to decay as SNR^{-1}. The same observations for extended targets and phased-array radars have also been made in [3] and [4], albeit for a different MIMO radar model and different detectors.

The remainder of the paper is organized as follows. Section II provides the MIMO radar system model. The statement of the composite detection problem and the definition of optimality are provided in Section III. We formulate and analyze the joint estimation and detection problem for MIMO radars for extended and point targets in Sections IV and V, respectively, and for phased-array radars in Section VI. The analysis on the diversity gain are presented in Section VII. Simulation results are illustrated in Sections VIII and IX provides the concluding remarks.

II. MIMO RADAR

We consider a MIMO radar system comprising of N_t and N_r transmit and receive antennas, respectively, and adopt the classical Swerling case I model [12] extended for multiple-antenna systems [3], [4]. According to this model, a target consists of one or more small scatterers exhibiting random, independent and isotropic scintillation.

We define P as the number of the target's scatterers and denote the locations of these scatterers in the Cartesian coordination by X_p for $p = 1, \ldots, P$. Also, we denote the reflectivity factor of the pth scatterer by ζ_p and assume that $\{\zeta_p\}_{p=1}^P$ are identically and independently distributed as zero-mean complex random variables with variance $1/P$. The target and reflectivity factors are assumed to remain constant during a finite number of observations denoted by K and change to independent states afterwards. Motivated by capturing the inherent diversity provided by independent scatterers, the antennas are spaced widely enough (such that they satisfy the conditions in [3, Sec. II.A]) to ensure that the received antennas capture uncorrelated reflections from the target. As illustrated in Fig. 1, we assume that the transmit antennas are located at X_m^t, for $m = 1, \ldots, N_t$, and the receive antennas are located at X_n^r, for $n = 1, \ldots, N_r$. The transmit antennas emit N_t *narrowband* waveforms of duration T with baseband equivalent models given by $\sqrt{(E/N_t)} s_m(t)$ for $m = 1, \ldots, N_t$, where E is the total transmitted energy and $\int_T |s_m(t)|^2 dt = 1$. In contrast to the conventional phased-array radars which deploy waveforms that are identical up to a scaling
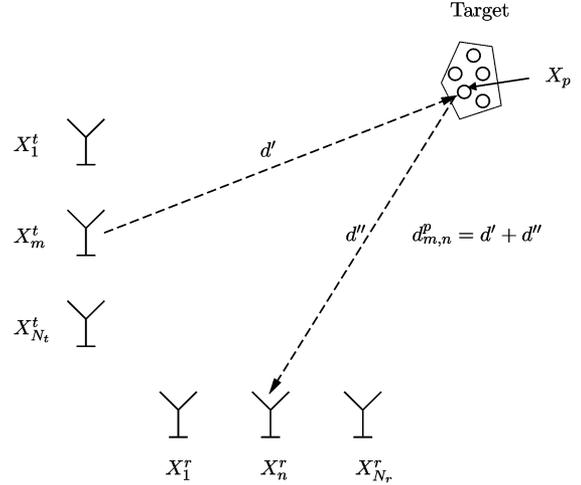

Fig. 1.   MIMO radar system.

factor [13], in MIMO radar systems these waveforms are designed such that they facilitate acquiring independent observations of each scatterer and often are assumed to be orthonormal [4], i.e.,

$$\forall\, m, n, \quad \int_T s_m(t) s_n^*(t) dt = \delta(m - n) \tag{1}$$

where $*$ denotes complex conjugate and $\delta(\cdot)$ is the Dirac's delta function. As depicted in Fig. 1, the waveform illuminated by the mth transmit antenna to the pth scatterer and received by the nth receive antenna passes through an end-to-end distance which we denote by $d_{m,n}^p$ and undergoes a time-delay which we denote by $\tau_{m,n}^p \triangleq d_{m,n}^p/c$, where c is the speed of light. By defining β as the path-loss exponent and superimposing the effects of all scatterers, the baseband equivalent of the signal received by the nth receive antenna due to the waveform $s_m(t)$ (transmitted by the mth transmit antenna) is given by

$$r_{m,n}(t) = \sqrt{\frac{E}{N_t}} \sum_{p=1}^P \zeta_p \left(\frac{1}{d_{m,n}^p} \right)^\beta s_m\!\left(t - \tau_{m,n}^p\right)$$
$$\times e^{-j2\pi f_c \tau_{m,n}^p} + z_{m,n}(t). \tag{2}$$

Note that this model differs from those of [3] and [4] in the sense that we have added the attenuation effects of path-losses by including the terms $\left((1/d_{m,n}^p)\right)^\beta = \left(\tau_{m,n}^p c\right)^{-\beta}$. The exponential term $\exp\left(-j2\pi f_c \tau_{m,n}^p\right)$ in (2) represents the effect of propagation phase shift, where f_c is the carrier frequency, and $z_{m,n}(t) \sim \mathcal{CN}(0, (1/N_t))$, denotes the additive white Gaussian noise.

We define X_0 as the location of the gravity center of the target and denote its associated time-delays and distances by $\{\tau_{m,n}\}$ and $\{d_{m,n}\}$, respectively. We assume that the distances $\{d_{m,n}\}$ are considerably larger than the dimensions of the object such that we can replace the distances and the time-delays associated with the scatterer X_p with those corresponding to the gravity center of the target X_0, i.e., $d_{m,n}^p = d_{m,n}$ and $\tau_{m,n}^p = \tau_{m,n}$, $\forall\, p$. Therefore,

$$s_m(t - \tau_{m,n}^p) = s_m(t - \tau_{m,n}), \quad \text{for } m = 1, \ldots, N_t,$$
$$n = 1, \ldots, N_r, \quad \text{and } p = 1, \ldots, P. \tag{3}$$

Using (2)–(3), the received signal at the nth antenna, which is a superposition of all emitted waveforms, is given by

$$
\begin{aligned}
r_n(t) &= \sqrt{\frac{E}{N_t}} \sum_{m=1}^{N_t} \sum_{p=1}^{P} \left(\frac{1}{d_{m,n}}\right)^{\beta} \zeta_p s_m(t - \tau_{m,n}) \\
&\quad \times e^{-j2\pi f_c \tau_{m,n}^p} + z_n(t) \\
&= \sqrt{\frac{E}{N_t}} \sum_{m=1}^{N_t} \frac{c^{-\beta}}{\tau_{m,n}^{\beta}} s_m(t - \tau_{m,n}) \\
&\quad \times \underbrace{\sum_{p=1}^{P} \zeta_p e^{-j2\pi f_c \tau_{m,n}^p}}_{\triangleq h_{m,n}} + z_n(t)
\end{aligned}
\tag{4}
$$

where $z_n(t) \triangleq \sum_{m=1}^{N_t} z_{m,n}(t) \sim \mathcal{CN}(0,1)$. Furthermore, we assume that the waveforms are narrowband. Based on the narrowband assumption we get [4]

$$
\begin{aligned}
\forall \ \tau, \quad s_m(t) &= e^{j2\pi f_c \tau} s_m(t - \tau), \\
\text{for } m &= 1, \ldots, N_t, \quad \text{and } n = 1, \ldots, N_r
\end{aligned}
\tag{5}
$$

which in conjunction with the orthonormality assumption (1) implies that

$$
\forall \ \tau_{m,k}, \tau_{n,k}, \quad \int_T s_m(t - \tau_{m,k}) s_n^*(t - \tau_{n,k}) dt = \delta(m - n).
\tag{6}
$$

We also define the time-delay vector $\boldsymbol{\tau} \triangleq [\tau_{1,1}, \ldots, \tau_{N_t, N_r}]$. Based on the model given in (2) and noting that the noise-terms $\{z_n(t)\}$ are unit-variance, the transmission signal-to-noise ratio, denoted by SNR, is given by SNR $= (E/T)$.

III. PROBLEM STATEMENT

We assume that the receive antennas sample the received signal at the rate of $1/T_s$ samples per second. By defining $r_n[k] \triangleq r_n(kT_s)$, $z_n[k] \triangleq z_n(kT_s)$, and $s_m[k; \tau] \triangleq s_m(kT_s - \tau)$, the discrete-time baseband equivalent of the received signal when a target is present is given by

$$
\begin{aligned}
r_n[k] &= \sqrt{\frac{E}{N_t}} c^{-\beta} \sum_{m=1}^{N_t} \frac{1}{\tau_{m,n}^{\beta}} h_{m,n} s_m[k; \tau_{m,n}] + z_n[k], \\
\text{for } k &= 1, \ldots, K.
\end{aligned}
\tag{7}
$$

We also assume that the sampling rate is high enough to ensure that the discrete-time signals $s_m[k; \tau_{m,n}]$ remain orthogonal for arbitrary delays $\tau_{m,l}, \tau_{n,l}$, i.e., $\sum_k s_m[k; \tau_{m,l}] s_n^*[k; \tau_{n,l}] = (1/T_s)\delta(m - n)$. Let us define $\boldsymbol{r}[k] \triangleq [r_1[k], \ldots, r_{N_r}[k]]^T$ for $k = 1, \ldots, K$ and $\boldsymbol{R} \triangleq [\boldsymbol{r}[1]^T, \ldots, \boldsymbol{r}[K]^T]^T$.

The target detection framework that we propose is different from the conventional target detection with MIMO radars. In conventional MIMO radars, e.g., [3] and references therein, the space is broken into small cells and the radar detects the presence of the target in a given cell. In such radar models, the location to be probed is given, which means that the corresponding time-delay vector $\boldsymbol{\tau}$ is also given. Therefore, the detection problem can be cast as testing whether a target exists at a given set of time-delays (cf. [3]). In contrast, our objective is to detect the presence of a target that lies in an unknown location and thereof has unknown corresponding time-delays. For this purpose we treat the time-delay vector $\boldsymbol{\tau}$ as the unknown parameter to be estimated and based on that we formulate the target detection problem. In other words we exploit $\boldsymbol{\tau}$ as an intermediate variable which we estimate for being able to carry out target detection. Therefore, in our framework the main objective of estimating the time-delays is to facilitate performing detection. As a minor application, such time-delays can also be exploited for estimating the location of the target. Such target localization, however, is not optimal and for achieving optimal target localization one needs to treat the target location as the unknown parameter of interest and deploy the same framework for carrying out joint target detection and target localization (instead of time-delay estimation).

Let $f_0(\boldsymbol{R})$ denote the probability density function (pdf) of the received signal when a target is not present. When a target is present, the pdf of the received signal depends on an unknown parameter $\boldsymbol{x}$ (in this paper, $\boldsymbol{x}$ is the vector of time-delays) and is denoted by $f_1(\boldsymbol{R} \mid \boldsymbol{x})$. Therefore, by defining the estimate of $\boldsymbol{x}$ by $\hat{\boldsymbol{x}}$, the detection part of the problem can be cast as

$$
\begin{cases}
\mathcal{H}_0 : & \boldsymbol{R} \sim f_0(\boldsymbol{R}) \\
\mathcal{H}_1 : & \boldsymbol{R} \sim f_1(\boldsymbol{R} | \hat{\boldsymbol{x}}).
\end{cases}
\tag{8}
$$

Our objective is to jointly characterize the estimator $\hat{\boldsymbol{x}}$ and find the test for deciding between the hypotheses $\mathcal{H}_0$ and $\mathcal{H}_1$. For this purpose we define and optimize a measure which combines estimation and detection accuracies. The underlying idea for performing such optimization is to deploy the notions of *randomized tests* and *randomized estimators*. For any given observation vector $\boldsymbol{R} \in \mathbb{C}^{|\boldsymbol{R}|}$ we assign complementary probability terms $\delta_0(\boldsymbol{R})$ and $\delta_1(\boldsymbol{R}) = 1 - \delta_0(\boldsymbol{R})$ to the hypotheses $\mathcal{H}_0$ and $\mathcal{H}_1$, respectively. In a randomized test, $\delta_i(\boldsymbol{R})$ for $i = 0, 1$ is the probability that hypothesis $\mathcal{H}_i$ is selected. Clearly deterministic tests are special cases of randomized tests where $\{\delta_i(\boldsymbol{R})\}$ take only the values 0 or 1. Whenever the decision is in favor of $\mathcal{H}_1$, we also have to estimate the unknown parameter $\boldsymbol{x}$. In deterministic approaches, the estimate of $\boldsymbol{x}$ is a deterministic function of the observed data. On the contrary, randomized estimators, instead of generating a deterministic value $\hat{\boldsymbol{x}}$, generate a random variable $\hat{\boldsymbol{x}}$ according to a distribution which is a function of the observed data. Deterministic estimators can be classified as a special case of randomized estimators.

We strive to identify the decision rules $\delta_0(\boldsymbol{R})$ and $\delta_1(\boldsymbol{R})$ such that the error in estimating $\boldsymbol{x}$, conditioned on the hypothesis $\mathcal{H}_1$ being true, is minimized. This minimization is also subject to an upper bound constraint on the false alarm probability $\Pr(\mathcal{H}_1 \mid \mathcal{H}_0)$. When the hypothesis $\mathcal{H}_1$ is true, there exist two types of errors in estimating $\boldsymbol{x}$. First, the test result can be correctly in favor of $\mathcal{H}_1$, but $\boldsymbol{x}$ is estimated erroneously, where we denote the cost function associated with such estimation error by $C(\hat{\boldsymbol{x}}, \boldsymbol{x})$. Second, the test output might be wrongly in favor of $\mathcal{H}_0$, which leads to misestimating $\boldsymbol{x}$ and results in an error cost which we denote by $C_0(\boldsymbol{x})$. Note that the cost function $C(\hat{\boldsymbol{x}}, \boldsymbol{x})$ can be selected arbitrarily. In this paper, we consider the mean-square error (MSE) cost given by $C(\hat{\boldsymbol{x}}, \boldsymbol{x}) = \|\hat{\boldsymbol{x}} - \boldsymbol{x}\|^2$ and $C_0(\boldsymbol{x}) = \|\boldsymbol{x}\|^2$.

Subject to a maximum tolerable level of false alarm probability P_{fa}, the estimation strategy which *minimizes the average cost* over all possible randomized estimators is given by

$$\mathcal{P}(\boldsymbol{R}) = \begin{cases} \min_{\{\delta_i(\boldsymbol{R})\}}, & \mathbb{E}_{\boldsymbol{R},\boldsymbol{x},\hat{\boldsymbol{x}}}\left[C(\hat{\boldsymbol{x}},\boldsymbol{x})|\mathcal{H}_1\right] + \mathbb{E}_{\boldsymbol{R},\boldsymbol{x}}\left[C_0(\boldsymbol{x})|\mathcal{H}_1\right] \\ \text{s.t.,} & \Pr\left(\mathcal{H}_1|\mathcal{H}_0\right) \leq P_{fa}. \end{cases}$$
(9)

The optimal hypothesis test (formalized by $\{\delta_i(\boldsymbol{R})\}$) and the optimal estimation strategy yielded by solving the problem $\mathcal{P}(\boldsymbol{R})$ for the choice of $C(\hat{\boldsymbol{x}},\boldsymbol{x}) = 0$ when $|\hat{\boldsymbol{x}} - \boldsymbol{x}| \leq \delta$ and 1 otherwise are described in the following theorem.

Theorem 1 (Moustakides [14]): For a finite cardinality vector $\boldsymbol{R} \in \mathbb{C}^{|\boldsymbol{R}|}$ and an unknown vector parameter $\boldsymbol{x} \in \mathcal{A}$, solving $\mathcal{P}(\boldsymbol{R})$ provides the optimal estimation strategy $\hat{\boldsymbol{x}}$ and the subsequent optimal detection rule for deciding between $\mathcal{H}_0$ and $\mathcal{H}_1$ are given by

$$\hat{\boldsymbol{x}} = \arg\max_{\boldsymbol{x} \in \mathcal{A}} \pi(\boldsymbol{x}) f_1(\boldsymbol{R}|\boldsymbol{x}), \quad \text{and} \quad \frac{f_1(\boldsymbol{R}|\hat{\boldsymbol{x}})}{f_0(\boldsymbol{R})} \overset{\mathcal{H}_1}{\underset{\mathcal{H}_0}{\gtrless}} \lambda \quad (10)$$

where $\pi(\boldsymbol{x})$ is the prior distribution of $\boldsymbol{x}$ and the estimation cost functions are $C(\hat{\boldsymbol{x}},\boldsymbol{x}) = 0$ when $|\hat{\boldsymbol{x}} - \boldsymbol{x}| \leq \delta$ and 1 otherwise.

The above theorem essentially establishes the GLRT as the optimal estimation/detection strategy with properties P1-P4 enumerated in the sequel. Several other *asymptotic* optimality results are known for the GLRT which are all based on having an *infinite* number of observation (cf. [14] and [15, Ch. 22]). $\hat{\boldsymbol{x}}$ given in (10) is the maximum *a posteriori* (MAP) estimate of $\boldsymbol{x}$. As we do not have any prior information about the parameter to be estimated (the vector of time-delays $\boldsymbol{\tau}$), throughout the analysis we assume that $\pi(\boldsymbol{x})$ has a uniform distribution. Hence, the MAP estimate of $\boldsymbol{x}$ becomes its ML estimate. The estimator and detector provided by Theorem 1 have the following properties.

P1) The ML estimator $\hat{\boldsymbol{x}}$ minimizes the *average* minimum-mean square estimation error of $\boldsymbol{x}$.

P2) The false alarm probability of the target detector is kept below a certain level.

P3) For the given set of ML estimates $\hat{\boldsymbol{x}}$, the target detector is Bayesian-optimal, i.e., the Bayes risk is minimized [16, Sec. II.B].

P4) The test requires only a finite number of samples, i.e., $|\boldsymbol{R}| < \infty$.

In order to apply the theorem above to our joint estimation/detection problem we set the vector of time-delays as the parameter to be estimated, i.e., $\boldsymbol{x} = \boldsymbol{\tau}$. For deploying the optimal estimator and detector provided in (10) we also need to characterize the domain of $\boldsymbol{x} = \boldsymbol{\tau}$ which in Theorem 1 is denoted by $\mathcal{A}$. Note that the vector $\boldsymbol{\tau}$ cannot be any arbitrary vector in the space $\mathbb{R}_+^{N_t N_r}$. This is due to the fact that for any given placement of antennas, there exists a correlation between the elements of $\boldsymbol{\tau}$ and there are some equations relating these time-delays. For the given antenna placements $\{X_m^t\}_{m=1}^{N_t}$ and $\{X_n^r\}_{n=1}^{N_r}$ let us define $\mathcal{X} \triangleq \{X_m^t, X_n^r\}$. Also for the given antenna placement $\mathcal{X}$ define $\mathcal{A}(\mathcal{X}) \subseteq \mathbb{R}_+^{N_t N_r}$ as the set which contains the vectors that can be valid choices for $\boldsymbol{\tau}$.

Precise characterization of $\mathcal{A}(\mathcal{X})$ is crucial for attaining the optimal estimation and detection performance. Any inaccuracy in such characterization degrades the performance and provides only *sub-optimal* estimators and detectors. In the sequel we provide necessary conditions for a given $\boldsymbol{\tau}$ to be a valid time-delay vector. Such necessary conditions describe a set of time-delay vectors which is a superset of $\mathcal{A}(\mathcal{X})$. We also *conjecture* that these conditions are sufficient which consequently can characterize $\mathcal{A}(\mathcal{X})$ precisely. If these conditions are not sufficient, then the resulting approximation of $\mathcal{A}(\mathcal{X})$ will only provide a *sub-optimal* solution.

For establishing the necessary conditions let us break down the end-to-end time-delay $\tau_{m,n}$ as $\tau_{m,n} = t_m + t'_n$, where t_m is the time required for the waveform to travel from the mth transmit antenna to the target and t'_n is the time required for the reflected waveform to travel from the target to the nth receive antenna. If a given $\boldsymbol{\tau}$ is a valid time-delay vector then $\forall\, m, i \in \{1, \ldots, N_t\}$ the three terms t_m, t_i, and $(\|X_m^t - X_i^t\|/c)$ should constitute the lengths of a triangle with its vertices given by the locations of the mth transmit antenna, the ith transmit antenna, and the target ($\|X_m^t - X_i^t\|$ is the distance between the mth and ith transmit antennas). The triangular inequalities impose that $\boldsymbol{\tau}$ is a valid time-delay vector only if

$$|t_m - t_i| \leq \frac{\|X_m^t - X_i^t\|}{c} \text{ for } m, i = 1, \ldots, N_t.$$

Similarly, by considering the triangles corresponding to the receive antennas we get the necessary conditions

$$|t'_n - t'_j| \leq \frac{\|X_n^r - X_j^r\|}{c} \text{ for } n, j = 1, \ldots, N_r.$$

By recalling that $\tau_{m,n} = t_m + t'_n \,\forall\, m, n, i, j$, we find that $|t_m - t_i| = |\tau_{m,n} - \tau_{i,n}|$ and $|t'_n - t'_j| = |\tau_{m,n} - \tau_{m,j}|$. Therefore, for the subspace $\mathcal{A}(\mathcal{X})$ we have

$$\mathcal{A}(\mathcal{X}) \subseteq \left\{ \boldsymbol{\tau} : |\tau_{m,n} - \tau_{i,n}| \leq \frac{\|X_m^t - X_i^t\|}{c}, \right.$$
$$\left. \text{and } |\tau_{m,n} - \tau_{m,j}| \leq \frac{\|X_n^r - X_j^r\|}{c} \,\forall\, m, i, j, n \right\}. \quad (11)$$

We conjecture that any vector $\boldsymbol{\tau}$ that satisfies the conditions above is a valid time-delay vector and therefor the subset operator $\subseteq$ can be replaced by equality. We underline that, however, in the case that these conditions are not sufficient, performing optimization on the above superset of $\mathcal{A}(\mathcal{X})$ will provide only *sub-optimal* estimators and detectors.

IV. JOINT DETECTION AND ESTIMATION FOR EXTENDED TARGETS

In this section, we consider the targets that are extended enough to be modeled as a group of isotropic and independent scatterers, i.e., $P \gg 1$ in (2). Our objective is to optimally detect a target, based on the model in (8), and simultaneously estimate the vector of time-delays $\boldsymbol{\tau}$. At the same time we assume that only a finite number of observations are available. According to Theorem 1 this problem can be solved via the GLRT given in (10) for $\boldsymbol{x} = \boldsymbol{\tau}$ and for $\mathcal{A} = \mathcal{A}(\mathcal{X})$ given in (11).

We start by deriving the ML estimate of $\boldsymbol{\tau}$ and then provide the detection-related analysis. We also develop a technique in Section VIII based on the Newton–Raphson method for localizing the target by using the estimated time-delay vector. Exploiting this simple target localization method is not the optimal

strategy and is merely intended to provide some numerical evaluations to show the improvement gained by deploying MIMO radars.

A. Time-Delay Estimation

The hypothesis given in (8) can be cast as

$$
\begin{cases}
\mathcal{H}_0: & r_n[k] = z_n[k] \\
\mathcal{H}_1: & r_n[k] = \sqrt{\frac{E}{N_t}} c^{-\beta} \sum_{m=1}^{N_t} \frac{1}{\tau_{m,n}^\beta} h_{m,n} s_m[k;\tau_{m,n}] + z_n[k].
\end{cases}
$$
(12)

Define $\boldsymbol{h} \triangleq [h_{1,1}, h_{1,2}, \ldots, h_{N_t,N_r}]^T$, where $h_{m,n}$, as defined in (4), accounts for the effects of the position and reflectiveness of the scatterers corresponding to the mth transmit and the nth receive antennas. The antennas are widely separated and the reflectivity factors $\{\zeta_p\}$ are complex and independently distributed with zero mean and variance $1/P$ with $P \gg 1$. Therefore, by using the central limit theorem, $\{h_{m,n}\}$ are i.i.d. and distributed as $\mathcal{CN}(0,1)$ [3].

Based on the model given in (7), when a target is present, the vector of the received signals $\boldsymbol{R}$ depends on the time-delays, which we are interested in estimating, as well as on the unknown random vector $\boldsymbol{h}$. Therefore, when a target is present, the pdf of $\boldsymbol{R}$ for any given $\boldsymbol{\tau}$ and $\boldsymbol{h}$ is $f_1(\boldsymbol{R} \mid \boldsymbol{\tau}, \boldsymbol{h})$. In order to obtain the ML estimate of $\boldsymbol{\tau}$ one approach is to estimate it through solving $\arg\max_{\boldsymbol{\tau} \in \mathcal{A}(\mathcal{X})} f_1(\boldsymbol{R} \mid \boldsymbol{\tau})$, which requires recovering $f_1(\boldsymbol{R} \mid \boldsymbol{\tau})$ from $f_1(\boldsymbol{R} \mid \boldsymbol{\tau}, \boldsymbol{h})$ by averaging over all realizations of $\boldsymbol{h}$. Alternatively, we can estimate it jointly with $\boldsymbol{h}$ when doing so is deemed to be beneficial. The latter approach is more beneficial when an accurate estimate of $\boldsymbol{h}$ is available, e.g., in the high SNR regimes, while averaging leads to a better performance when the estimate is very inaccurate, e.g., in the low SNR regimes. The ML estimate of $\boldsymbol{\tau}$ is provided in the following theorem for both scenarios.

Theorem 2: The ML estimate of $\boldsymbol{\tau}$ for extended targets and a given antenna placement $\mathcal{X}$:
1) through MAP estimation of $\boldsymbol{h}$ is given by

$$
\hat{\boldsymbol{\tau}}^{\mathrm{MAP}} = \arg\max_{\boldsymbol{\tau} \in \mathcal{A}(\mathcal{X})} \sum_{m=1}^{N_t} \sum_{n=1}^{N_r} \frac{\left| \sum_{k=1}^{K} r_n[k] s_m^*[k;\tau_{m,n}] \right|^2}{\frac{1}{T_s} + \frac{N_t}{E}(c\tau_{m,n})^{2\beta}}
$$

2) and through averaging over all realizations of $\boldsymbol{h}$ is given by

$$
\hat{\boldsymbol{\tau}}^{\mathrm{ave}} = \arg\max_{\boldsymbol{\tau} \in \mathcal{A}(\mathcal{X})} \sum_{m=1}^{N_t} \sum_{n=1}^{N_r} \Bigg\{ \frac{\left| \sum_{k=1}^{K} r_n[k] s_m^*[k;\tau_{m,n}] \right|^2}{\frac{1}{T_s} + \frac{N_t}{E}(c\tau_{m,n})^{2\beta}} - \log\left(\frac{E}{T_s N_t}(c\tau_{m,n})^{-2\beta} + 1 \right) \Bigg\}
$$

Proof: See Appendix A. ∎

B. Target Detection

Based on the ML estimates of the time-delay vector $\boldsymbol{\tau}$ provided in Theorem 2, we proceed to find the corresponding optimum detectors. We show that both estimates give rise to the same optimal detector given in the following lemma.

Lemma 1: The optimal test for extended targets and for the given estimate $\hat{\boldsymbol{\tau}}$ is

$$
\sum_{m=1}^{N_t} \sum_{n=1}^{N_r} \frac{\left| \sum_{k=1}^{K} r_n^*[k] s_m[k;\hat{\tau}_{m,n}] \right|^2}{\frac{E}{T_s N_t} + (c\hat{\tau}_{m,n})^{2\beta}} \underset{\mathcal{H}_0}{\overset{\mathcal{H}_1}{\gtrless}} \theta.
$$
(13)

Proof: Based on the model in (12) the likelihood $f_0(\boldsymbol{R})$ under the null hypothesis is given by

$$
f_0(\boldsymbol{R}) = (\pi)^{-KN_r} \exp\left(-\sum_k \|\boldsymbol{r}[k]\|^2 \right).
$$
(14)

Finding the estimate $\hat{\boldsymbol{\tau}}^{\mathrm{MAP}}$ is carried out by jointly estimating $\boldsymbol{\tau}$ and $\boldsymbol{h}$. For this estimate of $\boldsymbol{\tau}$, by setting $\boldsymbol{x} = [\boldsymbol{\tau}, \boldsymbol{h}]$ the optimal detector characterized in (10) is found as

$$
\frac{\max_{\boldsymbol{x} \in \mathcal{A}} \pi(\boldsymbol{x}) f_1(\boldsymbol{R}|\boldsymbol{x})}{f_0(\boldsymbol{R})} = \frac{\max_{\boldsymbol{\tau} \in \mathcal{A}(\mathcal{X}), \boldsymbol{h}} f_1(\boldsymbol{R}|\boldsymbol{\tau}, \boldsymbol{h}) f_{\boldsymbol{h}}(\boldsymbol{h})}{f_0(\boldsymbol{R})}
$$
$$
= \frac{f_1(\boldsymbol{R}|\hat{\tau}, \hat{\boldsymbol{h}}) f_{\boldsymbol{h}}(\hat{\boldsymbol{h}})}{f_0(\boldsymbol{R})} \underset{\mathcal{H}_0}{\overset{\mathcal{H}_1}{\gtrless}} \lambda
$$

where $\hat{\boldsymbol{\tau}}$ and $\hat{\boldsymbol{h}}$ are the MAP estimates obtained in Theorem 2. By following the same line of argument as in Appendix A (30)–(39) and recalling the definitions of $\boldsymbol{a}_{\boldsymbol{\tau}}$ and $\boldsymbol{B}_{\boldsymbol{\tau}}$ given in (32) and (35), respectively, the detector is given by (15)–(16), shown at the bottom of the page, where $\theta \triangleq (2N_t/E) \log \lambda$.

$$
\log\left(\frac{f_1(\boldsymbol{R}|\hat{\tau}, \hat{\boldsymbol{h}}) f_{\boldsymbol{h}}(\hat{\boldsymbol{h}})}{f_0(\boldsymbol{R})} \right) = \log\left(\frac{(\pi)^{-KN_r} \exp\left(-\sum_k \|\boldsymbol{r}[k]\|^2 \right) \exp\left(\boldsymbol{a}_{\hat{\boldsymbol{\tau}}}^H \boldsymbol{B}_{\hat{\boldsymbol{\tau}}}^{-1} \boldsymbol{a}_{\hat{\boldsymbol{\tau}}} \right)}{(\pi)^{-KN_r} \exp\left(-\sum_k \|\boldsymbol{r}[k]\|^2 \right)} \right)
$$
$$
= \boldsymbol{a}_{\hat{\boldsymbol{\tau}}}^H \boldsymbol{B}_{\hat{\boldsymbol{\tau}}}^{-1} \boldsymbol{a}_{\hat{\boldsymbol{\tau}}}
$$
(15)
$$
= \sum_{m=1}^{N_t} \sum_{n=1}^{N_r} \frac{\left| \sum_{k=1}^{K} r_n^*[k] s_m[k;\hat{\tau}_{m,n}] \right|^2}{\frac{E}{T_s N_t} + (c\hat{\tau}_{m,n})^{2\beta}} \underset{\mathcal{H}_0}{\overset{\mathcal{H}_1}{\gtrless}} \theta
$$
(16)

We further define $b_{m,n} \triangleq \sum_{k=1}^{K} r_n^*[k] s_m[k; \hat{\tau}_{m,n}]$ and $l_{m,n} \triangleq (E/T_s N_t) + (c\hat{\tau}_{m,n})^{2\beta}$. Therefore, the value of the threshold θ is linked to the probability of false alarm P_{fa} as

$$P_{fa} = P\left\{ \sum_{m=1}^{N_t} \sum_{n=1}^{N_r} \frac{|b_{m,n}|^2}{l_{m,n}} > \theta \Big| \mathcal{H}_0 \right\}.$$

Note that under $\mathcal{H}_0$, $b_{m,n}$ is distributed as $\mathcal{CN}(0, (1/T_s))$ and therefore, $|b_{m,n}|^2$ is exponentially distributed with parameter T_s. Hence, $\{|b_{m,n}|^2/l_{m,n}\}$ have exponential distributions with distinct parameters $T_s \cdot l_{m,n}^{-1}$. Thus, $\sum_m \sum_n (|b_{m,n}|^2/l_{m,n})$ is the sum of $N_t N_r$ independent exponential random variables with different parameters and its pdf is given by [17]

$$X \triangleq \sum_m \sum_n \frac{|b_{m,n}|^2}{l_{m,n}}$$
$$\sim \left[\prod_{m=1}^{N_t} \prod_{n=1}^{N_r} \frac{1}{T_s \cdot l_{m,n}} \right]$$
$$\times \sum_{m=1}^{N_t} \sum_{n=1}^{N_r} \frac{\exp\left(-T_s l_{m,n}^{-1} x\right)}{\prod_{i \neq m} \prod_{j \neq n} T_s \left(l_{i,j}^{-1} - l_{m,n}^{-1}\right)}. \quad (17)$$

If we denote the cumulative distribution function (CDF) of this random variable by $G_1(\cdot)$, then θ can be determined as $\theta = G_1^{-1}(1 - P_{fa})$. By following a similar line of analysis for the case that we deploy the estimate $\hat{\tau}^{\text{ave}}$, the same detector is found. ∎

It is noteworthy that our detection scheme has two major differences with that of [3] provided in [3, Eq. (24)]. First, the detector in [3, Eq. (24)] tests whether a target exists at a *known* time-delay while we try to detect a target with *unknown* time-delays. Second, the model of [3] embeds the effect of the time-delays only as *phase shifts* and ignores the *path-loss* effect. By recalling that the path-losses also depend on the time-delays we have modified the model of [3] to also capture the effects of path-losses.

V. JOINT DETECTION AND ESTIMATION FOR POINT TARGETS

In this section, we consider the application of MIMO radars for detecting point targets or exposing single-scatterers. In this case, the target is modeled by one scatterer located at its gravity center X_0. Note that in (4) by setting $P = 1$ we get $h_{m,n} = \zeta e^{-j2\pi f_c \tau_{m,n}}$. Unlike in extended targets, the previous section, the distribution of the reflectivity factor ζ is not known and thereof it should be treated as an unknown quantity to be estimated along with the time-delays. Therefore, the null and alternative hypotheses are given by

$$\begin{cases} \mathcal{H}_0: & r_n[k] = z_n[k] \\ \mathcal{H}_1: & r_n[k] = \sqrt{\frac{E}{N_t}} \zeta \sum_{m=1}^{N_t} \frac{c^{-\beta}}{\tau_{m,n}^{\beta}} s_m[k; \tau_{m,n}] e^{-j2\pi f_c \tau_{m,n}} + z_n[k]. \end{cases}$$
$$(18)$$

As before, we are interested in solving the optimum test given in (10) and we start by determining the ML estimates of the reflectivity ζ and the time-delay vector τ.

A. Time-Delay Estimation

Based on the model given in (18) and the fact that the distribution of ζ is not known *a priori*, we estimate τ along with ζ. The pdf of the received vector $\boldsymbol{R}$ for any given τ and ζ is $f_1(\boldsymbol{R} \mid \tau, \zeta)$. By setting $\boldsymbol{x} = [\tau, \zeta]$ and using the optimal test given in (10) the ML estimate of τ can be found as shown in the following theorem.

Theorem 3: The ML estimate of τ for point targets and antenna placement $\mathcal{X}$ is given by

$$\hat{\tau} = \arg \max_{\tau \in \mathcal{A}(\mathcal{X})} \frac{\left| \sum_{m=1}^{N_t} \sum_{n=1}^{N_r} \frac{e^{j2\pi f_c \tau_{m,n}}}{\tau_{m,n}^{\beta}} \sum_{k=1}^{K} r_n[k] s_m^*[k; \tau_{m,n}] \right|^2}{\sum_{m=1}^{N_t} \sum_{n=1}^{N_r} \frac{1}{\tau_{m,n}^{2\beta}}}.$$

Proof: See Appendix B. ∎

B. Target Detection

Based on the ML estimate of τ provided in Theorem 3 the optimal detector is characterized by the following lemma.

Lemma 2: The optimal test for point targets and for the given estimate $\hat{\tau}$ is

$$\left| \sum_{m=1}^{N_t} \sum_{n=1}^{N_r} \frac{e^{j2\pi f_c \hat{\tau}_{m,n}}}{\hat{\tau}_{m,n}^{\beta}} \sum_{k=1}^{K} r_n[k] s_m^*[k; \hat{\tau}_{m,n}] \right|^2 \underset{\mathcal{H}_0}{\overset{\mathcal{H}_1}{\gtrless}} \theta.$$

Proof: As we are estimating τ jointly with ζ, by setting $\boldsymbol{x} = [\tau, \zeta]$ and applying Theorem 1 the optimal detector is given by

$$\frac{\max_{\boldsymbol{x} \in \mathcal{A}} \pi(\boldsymbol{x}) f_1(\boldsymbol{R}|\boldsymbol{x})}{f_0(\boldsymbol{R})} = \frac{\max_{\tau \in \mathcal{A}(\mathcal{X}), \zeta} f_1(\boldsymbol{R}|\tau, \zeta)}{f_0(\boldsymbol{R})}$$
$$= \frac{f_1(\boldsymbol{R}|\hat{\tau}, \hat{\zeta})}{f_0(\boldsymbol{R})} \underset{\mathcal{H}_0}{\overset{\mathcal{H}_1}{\gtrless}} \lambda$$

By following the same line of argument as in Section IV-B and by using the estimates $\hat{\tau}$ and $\hat{\zeta}$ given in Theorem 3 and (44), respectively, the optimum test for a point target is given by (19), shown at the bottom of the page. Moreover, by setting $\theta \triangleq \left(\sum_{m=1}^{N_t} \sum_{n=1}^{N_r} (c\hat{\tau}_{m,n})^{-2\beta}/T_s \right) \log \lambda$, the test can be cast as

$$\left| \sum_{m=1}^{N_t} \sum_{n=1}^{N_r} \frac{e^{j2\pi f_c \hat{\tau}_{m,n}}}{\hat{\tau}_{m,n}^{\beta}} \sum_{k=1}^{K} r_n[k] s_m^*[k; \hat{\tau}_{m,n}] \right|^2 \underset{\mathcal{H}_0}{\overset{\mathcal{H}_1}{\gtrless}} \theta.$$

In order to determine the value of the threshold θ, note that $e^{j2\pi f_c \hat{\tau}_{m,n}} \sum_{k=1}^{K} r_n[k] s_m^*[k; \hat{\tau}_{m,n}]$ is distributed as $\mathcal{CN}(0, (1/T_s))$ under $\mathcal{H}_0$ and $\sum_{k=1}^{K} r_n[k] s_m^*[k; \hat{\tau}_{m,n}]$ is independent of $\sum_{k=1}^{K} r_{n'}[k] s_{m'}^*[k; \hat{\tau}_{m',n'}]$ for $m \neq m'$ or $n \neq n'$. As a result, under $\mathcal{H}_0$ we have

$$\sum_{m=1}^{N_t} \sum_{n=1}^{N_r} \frac{e^{j2\pi f_c \hat{\tau}_{m,n}}}{\hat{\tau}_{m,n}^{\beta}} \sum_{k=1}^{K} r_n[k] s_m^*[k; \hat{\tau}_{m,n}]$$

$$\sim \mathcal{CN}\left(0, \frac{1}{T_s} \sum_{m=1}^{N_t} \sum_{n=1}^{N_r} \frac{1}{\hat{\tau}_{m,n}^{2\beta}} \right)$$

and consequently

$$\left| \sum_{m=1}^{N_t} \sum_{n=1}^{N_r} \frac{e^{j2\pi f_c \hat{\tau}_{m,n}}}{\hat{\tau}_{m,n}^{\beta}} \sum_{k=1}^{K} r_n[k] s_m^*[k; \hat{\tau}_{m,n}] \right|^2$$

$$\sim \text{Exponential} \left(\frac{T_s}{\displaystyle\sum_{m=1}^{N_t} \sum_{n=1}^{N_r} \frac{1}{\hat{\tau}_{m,n}^{2\beta}}} \right).$$

Therefore, for a given value of P_{fa}, the threshold level θ is found as

$$\theta = \frac{1}{T_s} \sum_{m=1}^{N_t} \sum_{n=1}^{N_r} \frac{1}{\hat{\tau}_{m,n}^{2\beta}} \log \frac{1}{P_{fa}}. \qquad \blacksquare$$

VI. OPTIMAL JOINT ESTIMATION/DETECTION FOR PHASED-ARRAY RADAR

We will compare the performance of MIMO radars against that of conventional phased-array radar systems. A phased-array system utilizes an array of closely located antennas and therefore, the channel coefficients $h_{m,n}$ are fully correlated, i.e., $h_{m,n} = h$. For the case of extended targets h is distributed as $\mathcal{CN}(0, 1)$ and for point targets its distribution is unknown [3]. Moreover, all the emitted waveforms are equal up to a scaling factor, i.e., $s_m(t) = \hat{s}_m s(t)$ for $m = 1, \ldots, N_t$ such that $\sum_{m=1}^{N_t} |\hat{s}_m|^2 = N_t$ (for having the total transmitted energy equal to E). Therefore, by using (7) and the narrowband assumption, the system model is given by

$$r_n[k] = \sqrt{\frac{E}{N_t}} c^{-\beta} h s[k; \tau_{1,1}]$$
$$\times \sum_{m=1}^{N_t} \frac{1}{\tau_{m,n}^{\beta}} \hat{s}_m e^{j2\pi f_c(\tau_{1,1} - \tau_{m,n})} + z_n[k],$$
$$\text{for } k = 1, \ldots, K. \qquad (20)$$

The following lemma is instrumental to deriving the ML estimate of the time-delay vector.

Lemma 3: For any given set of functions $\{g_i(t)\}_{i=1}^{N}$ where $g_i(t) : \mathbb{R} \to \mathbb{C}$ and $\alpha, t \in \mathbb{R}$, we have

$$\max_{t_2, \ldots, t_N \in \mathbb{R}} \left| \sum_{i=1}^{N} e^{j\alpha t_i} g_i(t_1) \right| = \sum_{i=1}^{N} |g_i(t_1)|.$$

Proof: See Appendix C. $\qquad \blacksquare$

For the purpose of analyzing the diversity gains as given in Section VII, as well as comparing estimation performance, we provide the optimal detector and estimator for phased-array radars in the following lemmas. For further analysis we define $S_n(\boldsymbol{\tau}) \triangleq \sum_{m=1}^{N_t} (1/(c\tau_{m,n})^{\beta}) \hat{s}_m e^{j2\pi f_c(\tau_{1,1} - \tau_{m,n})}$ and $\hat{S}_n(\boldsymbol{\tau}) \triangleq \sum_{m=1}^{N_t} (1/(c\tau_{m,n})^{\beta}) \hat{s}_m e^{j2\pi f_c(\tau_{1,1} - 2\tau_{m,n})}$. Similar to $\mathcal{A}(\mathcal{X})$ which we defined for MIMO radars, we also define $\mathcal{A}'(\mathcal{X}')$ such that it contains the valid choices of the time-delays for a phased-array radar with closely located antenna placement $\mathcal{X}'$.

Lemma 4: For a given antenna placement $\mathcal{X}'$, the ML estimate of the time-delay vector $\boldsymbol{\tau}$ and the optimal detector in phased-array radars are as follows.

1) For extended targets through estimating h we have

$$\hat{\boldsymbol{\tau}}^{\text{MAP}} = \arg \max_{\boldsymbol{\tau} \in \mathcal{A}'(\mathcal{X}')} \frac{\left| \sum_{n=1}^{N_r} S_n^*(\boldsymbol{\tau}) \sum_{k=1}^{K} r_n[k] s^*[k; \tau_{1,1}] \right|^2}{\frac{1}{T_s} \sum_{n=1}^{N_r} |S_n(\boldsymbol{\tau})|^2 + 1}.$$

2) For extended targets through averaging over all realizations of h we have

$$\hat{\boldsymbol{\tau}}^{\text{ave}} = \arg \max_{\boldsymbol{\tau} \in \mathcal{A}'(\mathcal{X}')} \left\{ \frac{\left| \sum_{n=1}^{N_r} S_n^*(\boldsymbol{\tau}) \sum_{k=1}^{K} r_n[k] s^*[k; \tau_{1,1}] \right|^2}{\frac{1}{T_s} \sum_{N=1}^{N_r} |S_n(\boldsymbol{\tau})|^2 + \frac{N_t}{E}} \right.$$
$$\left. - \log \left(\frac{E}{T_s N_t} \sum_{n=1}^{N_r} |S_n(\boldsymbol{\tau})|^2 + 1 \right) \right\}.$$

3) For point targets through estimating ζ we have

$$\hat{\boldsymbol{\tau}} = \arg \max_{\boldsymbol{\tau} \in \mathcal{A}'(\mathcal{X}')} \frac{\left| \sum_{n=1}^{N_r} \hat{S}_n^*(\boldsymbol{\tau}) \sum_{k=1}^{K} r_n[k] s^*[k; \tau_{1,1}] \right|^2}{\frac{1}{T_s} \sum_{n=1}^{N_r} |\hat{S}_n(\boldsymbol{\tau})|^2}.$$

Proof: See Appendix D. $\qquad \blacksquare$

Based on the ML estimates of $\boldsymbol{\tau}$ provided in Lemma 4, the optimal detectors are presented in the following lemma.

Lemma 5: The optimal test for the given estimate $\boldsymbol{\tau}$ is given as follows.

$$\log \left(\frac{f_1(\boldsymbol{R} | \hat{\boldsymbol{\tau}}, \hat{\zeta})}{f_0(\boldsymbol{R})} \right) = \log \left(\frac{(\pi)^{-KN_r} \exp \left(-\sum_k \|\boldsymbol{r}[k]\|^2 \right) \exp \left(\frac{E}{T_s N_t} |\hat{\zeta}|^2 \sum_{m=1}^{N_t} \sum_{n=1}^{N_r} \frac{c^{-2\beta}}{\hat{\tau}_{m,n}^{2\beta}} \right)}{(\pi)^{-KN_r} \exp \left(-\sum_k \|\boldsymbol{r}[k]\|^2 \right)} \right)$$

$$= \frac{T_s \left| \sum_{m=1}^{N_t} \sum_{n=1}^{N_r} \frac{c^{-\beta}}{\hat{\tau}_{m,n}^{\beta}} e^{j2\pi f_c \hat{\tau}_{m,n}} \sum_{k=1}^{K} r_n[k] s_m^*[k; \hat{\tau}_{m,n}] \right|^2}{\sum_{m=1}^{N_t} \sum_{n=1}^{N_r} \frac{c^{-2\beta}}{\hat{\tau}_{m,n}^{2\beta}}} \underset{\mathcal{H}_0}{\overset{\mathcal{H}_1}{\gtrless}} \lambda. \qquad (19)$$

1) For extended targets

$$\left| \sum_{n=1}^{N_r} S_n^*(\boldsymbol{\tau}) \sum_{k=1}^{K} r_n[k] s^*[k; \hat{\tau}_{1,1}] \right|^2 \underset{\mathcal{H}_0}{\overset{\mathcal{H}_1}{\gtrless}} \hat{\theta}.$$

2) For point targets

$$\left| \sum_{n=1}^{N_r} \hat{S}_n^*(\boldsymbol{\tau}) \sum_{k=1}^{K} r_n[k] s^*[k; \hat{\tau}_{1,1}] \right|^2 \underset{\mathcal{H}_0}{\overset{\mathcal{H}_1}{\gtrless}} \hat{\theta}.$$

Proof: For the case that we are estimating $\boldsymbol{\tau}$ and h jointly, we set $\boldsymbol{x} = [\boldsymbol{\tau}, h]$ and therefore, the optimal detector is given by

$$\frac{\max_{\boldsymbol{x} \in \mathcal{A}} \pi(\boldsymbol{x}) f_1(\boldsymbol{R}|\boldsymbol{x})}{f_0(\boldsymbol{R})} = \frac{\max_{\boldsymbol{\tau} \in \mathcal{A}'(\mathcal{X}'), \boldsymbol{h}} f_1(\boldsymbol{R}|\boldsymbol{\tau}, \boldsymbol{h}) f_{\boldsymbol{h}}(\boldsymbol{h})}{f_0(\boldsymbol{R})}$$

$$= \frac{f_1(\boldsymbol{R}|\hat{\boldsymbol{\tau}}, \hat{\boldsymbol{h}}) f_{\boldsymbol{h}}(\hat{\boldsymbol{h}})}{f_0(\boldsymbol{R})} \underset{\mathcal{H}_0}{\overset{\mathcal{H}_1}{\gtrless}} \hat{\lambda}.$$

Proceeding with the same line of argument as in Section IV-B, the optimal test is given by

$$\frac{f_1(\boldsymbol{R}|\hat{\boldsymbol{\tau}}, \hat{\boldsymbol{h}}) f_{\boldsymbol{h}}(\hat{\boldsymbol{h}})}{f_0(\boldsymbol{R})}$$

$$= \exp \left\{ \frac{\left| \sum_{n=1}^{N_r} S_n^*(\hat{\boldsymbol{\tau}}) \sum_{k=1}^{K} r_n[k] s^*[k; \hat{\tau}_{1,1}] \right|^2}{\frac{1}{T_s} \sum_{n=1}^{N_r} |S_n^*(\hat{\boldsymbol{\tau}})|^2 + \frac{N_t}{E}} \right\}$$

$$\underset{\mathcal{H}_0}{\overset{\mathcal{H}_1}{\gtrless}} \hat{\lambda}$$

or equivalently

$$\left| \sum_{n=1}^{N_r} S_n^*(\hat{\boldsymbol{\tau}}) \sum_{k=1}^{K} r_n[k] s^*[k; \hat{\tau}_{1,1}] \right|^2 \underset{\mathcal{H}_0}{\overset{\mathcal{H}_1}{\gtrless}} \hat{\theta},$$

where

$$\hat{\theta} = \log \hat{\lambda} \cdot \left(\frac{1}{T_s} \sum_{n=1}^{N_r} |S_n^*(\hat{\boldsymbol{\tau}})|^2 + \frac{N_t}{E} \right).$$

Under $\mathcal{H}_0$, the term $S_n^*(\hat{\boldsymbol{\tau}}) \sum_{k=1}^{K} r_n[k] s^*[k; \hat{\tau}_{1,1}]$ is distributed as $\mathcal{CN}(0, (|S_n^*(\hat{\boldsymbol{\tau}})|^2/T_s))$ and $\sum_{k=1}^{K} r_n[k] s^*[k; \hat{\tau}_{1,1}]$ is independent of $\sum_{k=1}^{K} r_{n'}[k] s^*[k; \hat{\tau}_{1,1}]$ for $n \neq n'$. As a result, under $\mathcal{H}_0$ we have

$$\sum_{n=1}^{N_r} S_n^*(\hat{\boldsymbol{\tau}}) \sum_{k=1}^{K} r_n[k] s^*[k; \hat{\tau}_{1,1}] \sim \mathcal{CN}\left(0, \frac{1}{T_s} \sum_{n=1}^{N_r} |S_n(\hat{\boldsymbol{\tau}})|^2\right)$$

and consequently

$$\left| \sum_{n=1}^{N_r} S_n^*(\hat{\boldsymbol{\tau}}) \sum_{k=1}^{K} r_n[k] s^*[k; \hat{\tau}_{1,1}] \right|^2$$

$$\sim \text{Exponential}\left(\frac{T_s}{\sum_{n=1}^{N_r} |S_n(\hat{\boldsymbol{\tau}})|^2} \right).$$

Therefore, for a given value of P_{fa}, the threshold level θ is found by

$$\theta = \frac{1}{T_s} \sum_{n=1}^{N_r} |S_n(\hat{\boldsymbol{\tau}})|^2 \log \frac{1}{P_{fa}}.$$

We can similarly find the same detector when the estimate $\hat{\boldsymbol{\tau}}^{\text{ave}}$ is computed by averaging out the effect of h. ∎

VII. DIVERSITY GAIN ANALYSIS

In order to compare the performance of MIMO and phased-array radars quantitatively, we analyze the diversity gain, which determines how fast the mis-detection probability decays as the transmission SNR increases while there is an upper-bound constraint on the false alarm probability [4]. More specifically we are interested in finding

$$d = -\lim_{\text{SNR} \to \infty} \frac{\log P_{md}(\text{SNR})}{\log \text{SNR}}$$

where $P_{md}(\text{SNR})$ denotes the mis-detection probability at the signal-to-noise ratio SNR. The diversity gain for the MIMO radar model provided in [3] has also been examined in [3], [4]. [3] also analyzes another notion of diversity, which is the asymptotic value of the detectors's divergence.

Throughout the analysis in the sequel, we say two functions $f_1(x)$ and $f_2(x)$ are *asymptotically equal* when $\lim_{x \to \infty} (f_1(x)/f_2(x)) = 1$ and denote it by $f_1(x) \overset{\circ}{=} f_2(x)$. We also define $\overset{\circ}{\leq}$ and $\overset{\circ}{\geq}$ accordingly. We also say two functions $f_1(x)$ and $f_2(x)$ are *exponentially equal* when $\lim_{x \to \infty} (\log f_1(x)/\log f_2(x)) = 1$ and denote it by $f_1(x) \doteq f_2(x)$.

Remark 1: Asymptotic equality is a sufficient condition for exponential equality.

We will use the following lemma for analyzing the diversity gain of MIMO and phased-array radars.

Lemma 6: For any M independent Gaussian random variables $Y_m \sim \mathcal{N}(\rho \cdot \mu_m, \sigma^2)$, $m = 1, \ldots, M$, where $\rho \in \mathbb{R}^+$ and $\mu_m \sim \mathcal{N}(0, \sigma_m^2)$, and for any given $\gamma \in \mathbb{R}^+$, in the asymptote of large values of ρ we have

$$\mathbb{E}_{\boldsymbol{\mu}}\left[\Pr\left(\sum_{m=1}^{M} Y_m^2 < \gamma \right) \right] \doteq \rho^{-M} \qquad (21)$$

where $\boldsymbol{\mu} \triangleq [\mu_1, \ldots, \mu_M]$.

Proof: See Appendix E. ∎

By using the lemma above, in the following theorem we establish the diversity gain achieved by MIMO and phased-array radars for both extended and point targets. $P_{md}(\text{SNR})$.

Theorem 4: The diversity gain achieved by the following:

1) an $N_t \times N_r$ MIMO radar system for extended targets is $N_t N_r$, i.e., $P_{md}^{\text{E}}(\text{SNR}) \doteq \text{SNR}^{-N_t N_r}$;

2) an $N_t \times N_r$ MIMO radar system for point targets is 1, i.e., $P_{md}^{P}(\text{SNR}) \doteq \text{SNR}^{-1}$;

3) an $N_t \times N_r$ phased-array system for extended and point targets is 1, i.e., $P_{md}^{\text{PA}}(\text{SNR}) \doteq \text{SNR}^{-1}$.

Proof:

1) For extended targets, by recalling the definitions of $b_{m,n} = \sum_{k=1}^{K} r_n^*[k] s_m[k; \hat{\tau}_{m,n}]$ and $l_{m,n} =$

$(E/T_s N_t) + (c\hat{\tau}_{m,n})^{2\beta}$, from the optimal test in (13) we have

$$P_{md}^{\mathrm{E}}(\mathrm{SNR}) = \mathrm{Pr}\left(\sum_{m=1}^{N_t}\sum_{n=1}^{N_r}\frac{|b_{m,n}|^2}{l_{m,n}} < \theta \Big| \mathcal{H}_1\right). \qquad (22)$$

We define $b_{m,n}^r \triangleq \Re(b_{m,n})$, $b_{m,n}^i \triangleq \Im(b_{m,n})$. Therefore, the mis-detection probability given in (22) is equivalently given by

$$P_{md}^{\mathrm{E}}(\mathrm{SNR}) = \mathrm{Pr}\left(\sum_{m=1}^{N_t}\sum_{n=1}^{N_r}\frac{1}{l_{m,n}}\left[(b_{m,n}^r)^2 + (b_{m,n}^i)^2\right]\right.$$
$$\left. < \theta \Big| \mathcal{H}_1\right). \quad (23)$$

By further defining $l_{\min} = \min_{m,n} l_{m,n}$ and $l_{\max} = \max_{m,n} l_{m,n}$ we can provide the following upper and lower bounds on the probability in (23)

$$\mathrm{Pr}\left(\sum_{m=1}^{N_t}\sum_{n=1}^{N_r}(b_{m,n}^r)^2 + (b_{m,n}^i)^2 < \theta l_{\min} \Big| \mathcal{H}_1\right)$$
$$\leq P_{md}^{\mathrm{E}}(\mathrm{SNR})$$
$$\leq \mathrm{Pr}\left(\sum_{m=1}^{N_t}\sum_{n=1}^{N_r}(b_{m,n}^r)^2 + (b_{m,n}^i)^2 < \theta l_{\max} \Big| \mathcal{H}_1\right). \qquad (24)$$

On the other hand, under hypothesis $\mathcal{H}_1$ from (12) we have

$$b_{m,n} = \sqrt{\frac{E}{N_t}}c^{-\beta}\sum_{m'=1}^{N_t}\frac{1}{\tau_{m',n}^\beta}h_{m',n}$$
$$\times\underbrace{\sum_{k=1}^{K}s_{m'}[k;\tau_{m',n}]s_m[k;\hat{\tau}_{m,n}]}_{(1/T_s)\delta(m-m')} + \underbrace{\sum_{k=1}^{K}z_n[k]s_m[k;\hat{\tau}_{m,n}]}_{\sim\mathcal{CN}(0,(1/T_s))}$$

which in turn provides

$$b_{m,n} \sim \mathcal{CN}\left(\sqrt{\frac{E}{N_t}}(c\tau_{m,n})^{-\beta}\cdot\frac{h_{m,n}}{T_s}, \frac{1}{T_s}\right).$$

Furthermore, by defining $h_{m,n}^r \triangleq \Re(h_{m,n})$ and $h_{m,n}^i \triangleq \Im(h_{m,n})$ we have $h_{m,n}^r, h_{m,n}^i \sim \mathcal{N}(0,(1/2))$ and

$$b_{m,n}^r \sim \mathcal{N}\left(\sqrt{\frac{E}{N_t}}(c\tau_{m,n})^{-\beta}\cdot\frac{h_{m,n}^r}{T_s}, \frac{1}{2T_s}\right)$$

and $b_{m,n}^i \sim \mathcal{N}\left(\sqrt{\frac{E}{N_t}}(c\tau_{m,n})^{-\beta}\cdot\frac{h_{m,n}^i}{T_s}, \frac{1}{2T_s}\right).$

Now, we apply Lemma 6 by setting $M = 2N_t N_r$, $\{Y_m\}_m = \{b_{m,n}^r, b_{m,n}^i\}_{m,n}$, $\rho = \sqrt{E}$, $\{\mu_m\}_m =$

$\sqrt{(1/N_t)}(c\tau_{m,n})^{-\beta} \times \{h_{m,n}^r, h_{m,n}^i\}$, $\sigma^2 = (1/2T)$ and $\sigma_\mu^2 = (1/2)$. Thus, we get $\forall \gamma$

$$\mathrm{Pr}\left(\sum_{m=1}^{N_t}\sum_{n=1}^{N_r}(b_{m,n}^r)^2 + (b_{m,n}^i)^2 < \gamma \Big| \mathcal{H}_1\right)$$
$$\doteq (\sqrt{E})^{-2N_t N_r} = (T_s\mathrm{SNR})^{-N_t N_r}$$
$$\doteq \mathrm{SNR}^{-N_t N_r}.$$

Hence, for the choices of $\gamma = \theta l_{\min}$ and $\gamma = \theta l_{\max}$ we find that the lower and upper bounds on $P_{md}^{\mathrm{E}}(\mathrm{SNR})$ given in (24) are both exponentially equal to $\mathrm{SNR}^{-N_t N_r}$. This results in an identical exponential order for $P_{md}^{\mathrm{E}}(\mathrm{SNR})$, i.e.,

$$P_{md}^{\mathrm{E}}(\mathrm{SNR}) \doteq \mathrm{SNR}^{-N_t N_r}$$

which establishes the desired result for MIMO radars with extended targets.

2) We define

$$\tilde{b} \triangleq \sum_{m=1}^{N_t}\sum_{n=1}^{N_r}\frac{e^{j2\pi f_c\hat{\tau}_{m,n}}}{\hat{\tau}_{m,n}^\beta}\sum_{k=1}^{K}r_n[k]s_m^*[k;\hat{\tau}_{m,n}]$$
$$= \sum_{m=1}^{N_t}\sum_{n=1}^{N_r}\frac{e^{j2\pi f_c\hat{\tau}_{m,n}}}{\hat{\tau}_{m,n}^\beta}\sqrt{\frac{E}{N_t}}\zeta c^{-\beta}\sum_{m'=1}^{N_t}\frac{e^{-j2\pi f_c\tau_{m',n}}}{\tau_{m',n}^\beta}$$
$$\times\underbrace{\sum_{k=1}^{K}s_{m'}[k;\tau_{m',n}]s_m^*[k;\hat{\tau}_{m,n}]}_{=(1/T_s)\delta(m-m')}$$
$$+\underbrace{\sum_{m=1}^{N_t}\sum_{n=1}^{N_r}\frac{e^{j2\pi f_c\hat{\tau}_{m,n}}}{\hat{\tau}_{m,n}^\beta}\sum_{k=1}^{K}z_n[k]s_m^*[k;\hat{\tau}_{m,n}]}_{\sim\mathcal{CN}\left(0, \sum_{m=1}^{N_t}\sum_{n=1}^{N_r}(1/T_s\hat{\tau}_{m,n}^{2\beta})\right)}.$$

Therefore, $\tilde{b}$ is distributed as

$$\tilde{b} \sim \mathcal{CN}\left(\sqrt{\frac{E}{N_t}}c^{-\beta}\sum_{m=1}^{N_t}\sum_{n=1}^{N_r}\frac{e^{j2\pi f_c(\hat{\tau}_{m,n}-\tau_{m,n})}}{(\hat{\tau}_{m,n}\tau_{m,n})^\beta}\right.$$
$$\left.\cdot\frac{\zeta}{T_s}, \sum_{m=1}^{N_t}\sum_{n=1}^{N_r}\frac{1}{T_s\hat{\tau}_{m,n}^{2\beta}}\right).$$

By following a similar line of argument as for extended targets and defining $\tilde{b}^r \triangleq \Re(\tilde{b})$, $\tilde{b}^i \triangleq \Im(\tilde{b})$ and

$$\zeta^r \triangleq \Re\left(\sum_{m=1}^{N_t}\sum_{n=1}^{N_r}\frac{e^{j2\pi f_c(\hat{\tau}_{m,n}-\tau_{m,n})}}{(\hat{\tau}_{m,n}\tau_{m,n})^\beta}\zeta\right),$$

$$\zeta^i \triangleq \Im\left(\sum_{m=1}^{N_t}\sum_{n=1}^{N_r}\frac{e^{j2\pi f_c(\hat{\tau}_{m,n}-\tau_{m,n})}}{(\hat{\tau}_{m,n}\tau_{m,n})^\beta}\zeta\right)$$

we get

$$\tilde{b}^r \sim \mathcal{N}\left(\sqrt{\frac{E}{N_t}}c^{-\beta} \cdot \frac{\zeta^r}{T_s}, \sum_{m=1}^{N_t}\sum_{n=1}^{N_r}\frac{1}{2T_s\hat{\tau}_{m,n}^{2\beta}}\right),$$

$$\text{and } \tilde{b}^i \sim \mathcal{N}\left(\sqrt{\frac{E}{N_t}}c^{-\beta} \cdot \frac{\zeta^i}{T_s}, \sum_{m=1}^{N_t}\sum_{n=1}^{N_r}\frac{1}{2T_s\hat{\tau}_{m,n}^{2\beta}}\right),$$

and

$$P_{md}^P(\text{SNR}) = \Pr\left(|\tilde{b}|^2 < \theta\right) = \Pr\left((\tilde{b}^r)^2 + (\tilde{b}^i)^2 < \theta\right).$$

Now, we apply Lemma 6 by setting $M = 2$, $\{Y_m\}_m = \{\tilde{b}^r, \tilde{b}^i\}$, $\rho = \sqrt{E}$, $\{\mu_m\}_m = \sqrt{(1/N_t)}c^{-\beta} \times \{\zeta^r, \zeta^i\}$, $\sigma^2 = (1/2T)$ and $\sigma_1^2 = \mathbb{E}[(\zeta^r)^2]$, $\sigma_2^2 = \mathbb{E}[(\zeta^i)^2]$. Therefore,

$$P_{md}^P(\text{SNR}) \doteq (\sqrt{E})^{-2} = (T_s\text{ssrSNR})^{-1} \doteq \text{SNR}^{-1}.$$

3) We provide the proof for extended targets. Similar line of argument and appropriate modifications provide the proof for point targets. Based on the optimal test for detecting extended targets by phased-array radars given in Lemma 5 we have

$$P_{md}^{\text{PA}} = \Pr\left(\left|\sum_{n=1}^{N_r} S_n^*(\hat{\tau})\sum_{k=1}^{K} r_n[k]s^*[k;\hat{\tau}_{1,1}]\right|^2 < \theta \Big| \mathcal{H}_1\right).$$

Under hypothesis $\mathcal{H}_1$ from (20) for extended targets we have

$$\hat{b} \triangleq \sum_{n=1}^{N_r} S_n^*(\hat{\tau})\sum_{k=1}^{K} r_n[k]s^*[k;\hat{\tau}_{1,1}]$$

$$= \sqrt{\frac{E}{N_t}}\underbrace{\sum_{n=1}^{N_r} S_n^*(\hat{\tau})S_n(\boldsymbol{\tau})h}_{\triangleq \hat{h}}\underbrace{\sum_{k=1}^{K} s[k;\tau]s^*[k;\hat{\tau}]}_{(1/T_s)}$$

$$+ \underbrace{\sum_{n=1}^{N_r}\sum_{k=1}^{K} z_n[k]s^*[k;\hat{\tau}]}_{\sim \mathcal{CN}(0,(N_r/T_s))}$$

where $h \sim \mathcal{CN}\left(0, |\sum_{n=1}^{N_r} S_n^*(\hat{\tau})S_n(\boldsymbol{\tau})|^2\right)$. Therefore,

$$\hat{b} \sim \mathcal{CN}\left(\sqrt{\frac{E}{N_t}} \cdot \frac{\hat{h}}{T_s}, \frac{N_r}{T_s}\right).$$

Similarly as before we define $\hat{b}^r \triangleq \Re(\hat{b})$, $\hat{b}^i \triangleq \Im(\hat{b})$, $\hat{h}^r \triangleq \Re(\hat{h})$ and $\hat{h}^i \triangleq \Im(\hat{h})$, where we have $\hat{h}^r, \hat{h}^i \sim \mathcal{CN}(0, (|\sum_{n=1}^{N_r} S_n^*(\hat{\tau})S_n(\boldsymbol{\tau})|^2/2))$ and

$$\hat{b}^r \sim \mathcal{CN}\left(\sqrt{\frac{E}{N_t}} \cdot \frac{\hat{h}^r}{T_s}, \frac{N_r}{2T}\right)$$

$$\text{and } \hat{b}^i \sim \mathcal{CN}\left(\sqrt{\frac{E}{N_t}} \cdot \frac{\hat{h}^i}{T_s}, \frac{N_r}{2T}\right).$$

Again we apply Lemma 6 by setting $M = 2$, $\{Y_1, Y_2\}_m = \{\hat{b}^r, \hat{b}^i\}$, $\rho = \sqrt{E}$, $\{\mu_1, \mu_2\}_m = \sqrt{(1/N_t)}(c\tau)^{-\beta} \times$

$\{\hat{h}^r, \hat{h}^i\}$, $\sigma^2 = (N_r/2T)$ and $\sigma_m^2 = (N_tN_r/2)$. Thus, we get $\forall \gamma$

$$\Pr\left((\hat{b}^r)^2 + (\hat{b}^i)^2 < \gamma\right) \doteq (\sqrt{E})^{-2} = \text{SNR}^{-1}.$$

As a result we find the following diversity gain achieved by phased-array radar systems for extended targets

$$P_{md}^{\text{PA}}(\text{SNR}) \doteq \text{SNR}^{-1}.$$

∎

Although we are using a MIMO radar model different from [3] and subsequently derive a different detector, the results above conform with those of [3] which considers detecting the presence of a target at a given location. This result demonstrates that in terms of diversity gain, our proposed MIMO radar model is capable of capturing the same diversity gain achieved by the MIMO radar model of [3].

VIII. SIMULATION RESULTS

A. Extended Targets

In this section, we provide simulation results on the performance of the proposed joint estimation/detection framework. We consider two antenna configurations with $N_t = N_r = 2$ and $N_t = 4$, $N_r = 8$. For the MIMO radar we assume that the transmit and receive antennas are located at $X_m^t = (m, 0, 0)$ for $m = 1, \ldots, 4$ and $X_n^r = (0, n, 0)$ for $n = 1, \ldots, 8$, respectively. For the phased-array radar we assume that the transmit antennas are all closely located around $X_m^t = (1, 0, 0)$ for $m = 1, \ldots, 4$, and the receive antennas are closely located around $X_n^r = (0, 1, 0)$ for $n = 1, \ldots, 8$. Also we assume that the target to be detected is located at $X_0 = (20, 15, 0)$, where all the distances are in kilometer (km). The path loss coefficient is $\beta = 2$ and the carrier frequency is $f_c = 5$ MHz. We assume that the target comprises of $P = 10$ scatterers and the number of signal samples is $K = 40$. Finally, for the MIMO radar the emitted waveforms are $s_m(t) = (1/\sqrt{T})\exp(j2\pi mt/T)(U(t) - U(t - T))$, where $U(t)$ is the unit step function and T denotes the duration of the waveform and the sampling rate at the receiver is $T_s = (T/10)$. For the phased-array radar all the emitted waveforms are equal to $s_1(t)$.

We first consider the performance of parameter estimation. Fig. 2 depicts the average normalized mean-square errors (MSE), i.e., $(1/N_tN_r)\sum_m\sum_n|(\hat{\tau}_{m,n} - \tau_{m,n})/\tau_{m,n}|^2$, for phased-array and MIMO radars as a function of received SNR. It is observed that the MIMO radar outperforms the phased-array in all SNR regimes and in particular, by a large margin in the low SNR regime, which is of more interest in radar applications. Moreover, it is seen that in MIMO radars, the MAP estimator $\hat{\tau}^{\text{MAP}}$ performs better than the estimator $\hat{\tau}^{\text{ave}}$ in the high SNR regime, while the estimator $\hat{\tau}^{\text{ave}}$ outperforms the MAP estimator $\hat{\tau}^{\text{MAP}}$ in the low SNR regime, as expected and discussed in Section IV-A.

It should be noted that comparing the accuracies of the time-delay estimators are not as informative as comparing the accuracies of the detectors. This is mainly because the time-delay estimates have different roles in MIMO and phased-array radars.
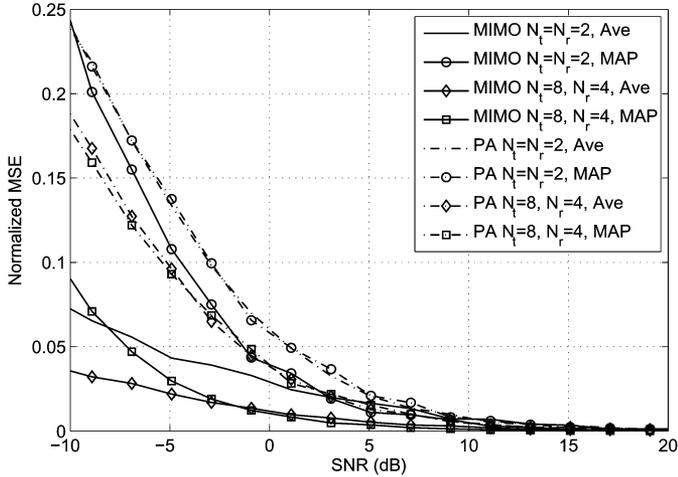
Fig. 2. Average normalized MSE of time-delay estimates versus SNR for extended targets.
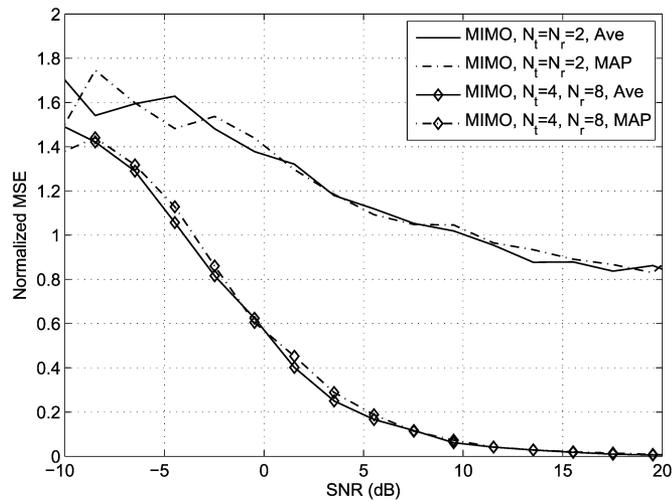

Fig. 3. Average normalized MSE of location estimates versus SNR for extended targets.

Nevertheless, we perform such comparisons as the detectors accuracies in our formulations depend on the estimators accuracies, which justifies comparing the time-delay estimator in MIMO and phased-array radars.

We next illustrate the localization performance of MIMO radar in Fig. 3. Once the vector $\hat{\boldsymbol{\tau}}$ is available, it is then possible to further estimate the location X_0 of the gravity center of the target. The localization problem can be formulated in the form of the following nonlinear equations:

$$\hat{\boldsymbol{\tau}} = \boldsymbol{\phi}(X_0) + \boldsymbol{\omega} \qquad (25)$$

where $\boldsymbol{\omega}$ is the noise term, and $\boldsymbol{\phi}(X_0) = [\phi_{1,1}(X_0), \ldots, \phi_{N_t,N_r}(X_0)]$ is the vector of functions defined as

$$\phi_{m,n}(X_0) \triangleq \frac{1}{c} \left(\|X_0 - X_m^t\| + \|X_0 - X_n^r\| \right),$$
$$m = 1, \ldots, N_t, \quad n = 1, \ldots, N_r \qquad (26)$$

where X_m^t and X_n^r are the positions of the mth and nth transmit and receive antennas, respectively. We can solve for X_0 from
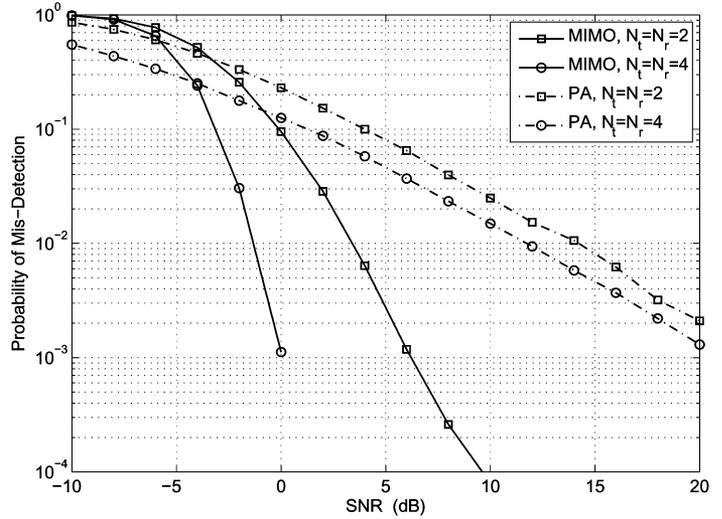

Fig. 4. Probability of mis-detection versus SNR for a false alarm $P_{fa} = 10^{-6}$ for extended targets.

(25) iteratively as follows. Denote $X_0^{(i)}$ as the solution at the ith iteration. By linearizing $\boldsymbol{\phi}(X_0^{(i+1)})$ with respect to $X_0^{(i)}$ we get

$$\boldsymbol{\phi}\left(X_0^{(i+1)}\right) \approx \boldsymbol{\phi}\left(X_0^{(i)}\right) + \boldsymbol{H}_0\left(X_0^{(i)}\right)\left(X_0^{(i+1)} - X_0^{(i)}\right) \tag{27}$$

where $\boldsymbol{H}_0\left(X_0^{(i)}\right)$ is the Jacobian of the function $\boldsymbol{\phi}(\cdot)$ evaluated at $X_0^{(i)}$. Then, the least-square estimate of the position X_0 based on (25) and (27) is given by

$$X_0^{(i+1)} = \arg\min_{X_0} \left[\boldsymbol{y}(X_0^{(i)}) - \boldsymbol{H}_0(X_0^{(i)})X_0 \right]^T$$
$$\cdot \left[\boldsymbol{y}(X_0^{(i)}) - \boldsymbol{H}_0(X_0^{(i)})X_0 \right] \qquad (28)$$

where $\boldsymbol{y}\left(X_0^{(i)}\right) \triangleq \boldsymbol{\tau} - \left(\boldsymbol{\phi}(X_0^{(i)}) - \boldsymbol{H}_0 X_0^{(i)}\right)$ and therefore $X_0^{(i+1)}$ has to satisfy the normal equation

$$\left[\boldsymbol{H}_0\left(X_0^{(i)}\right)^T \boldsymbol{H}_0\left(X_0^{(i)}\right)\right] X_0^{(i+1)} = \boldsymbol{H}_0\left(X_0^{(i)}\right)^T \boldsymbol{y}\left(X_0^{(i)}\right). \tag{29}$$

An initial estimate $X_0^{(0)}$ can be obtained, e.g., using the method in [18]. It is seen that the 4×8 MIMO radar performs considerably better than the 2×2 MIMO radar, which is due to the fact that 32 time-delays provide much more information about the position of the target than four time-delays do.

Finally we consider the detection performance. In Fig. 4, the probability of mis-detection versus SNR is illustrated. The tests are designed such that the probability of false alarm is $P_{fa} \leq 10^{-6}$. As analyzed in Section VII and observed in this figure, the slope of the mis-detection probability of the phased-array radar is 1 decade per 10 dB, whereas that of the MIMO radar is $N_t N_r$ times steeper. Fig. 5 shows the receiver operating curve (ROC) for the MIMO and the phased-array systems, for SNR $= 0$ dB. It is seen that the MIMO radar significantly outperforms the phased-array radar over a wide range of false alarm values.

B. Point Targets

We use a similar system setup as in Section VIII-A. Fig. 6 illustrates the normalized average MSE in estimating the time-de-
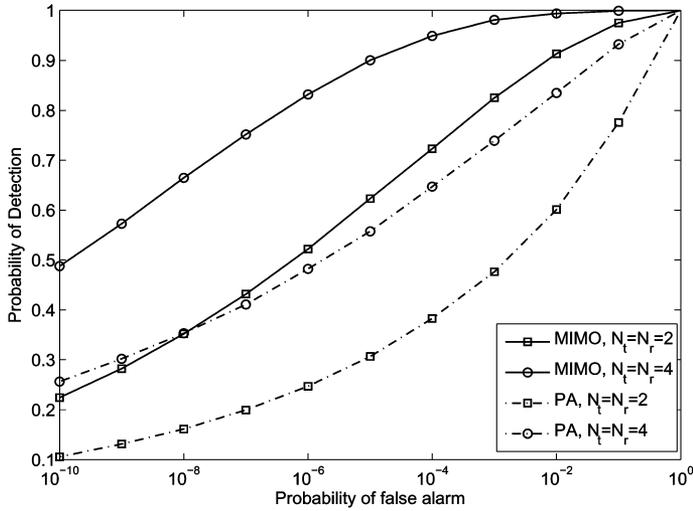
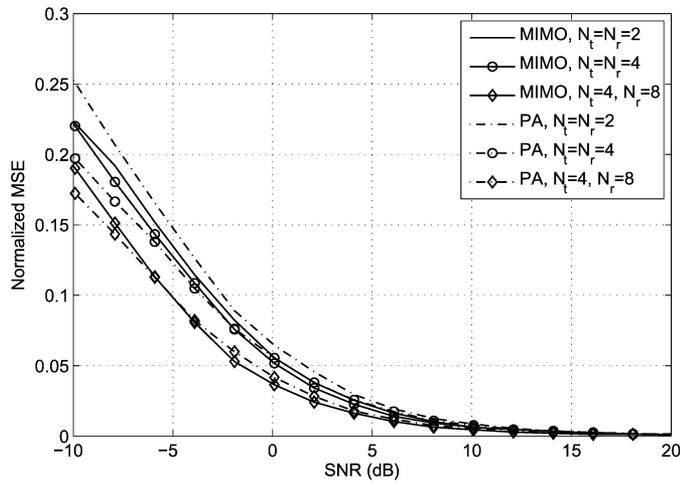Fig. 5. Probability of target detection versus probability of false alarm for SNR = 0 dB for extended targets.

Fig. 7. Probability of mis-detection versus SNR for point targets and $P_{fa} = 10^{-6}$ for point targets.

Fig. 6. Average normalized MSE of time-delay estimates versus SNR for point targets.

Fig. 8. Probability of target detection versus probability of false alarm for point targets and SNR = 0 dB for point targets.

lays versus SNR. Unlike for extended targets, it is observed that for point targets, conventional phased-array and MIMO radars exhibit similar target detection and time-delay estimation accuracies. Therefore, when considering joint target detection and time-delay estimation, deploying MIMO radars are not much advantageous for point targets. This conclusion is nevertheless limited to the specific problem analyzed in this paper and MIMO radars can be potentially advantageous in other scenarios like those discussed in [4] and references therein. This is due to the fact that point targets lack independent scattering section and thereof provide no diversity gain.

In Figs. 7 and 8, the probability of mis-detection versus SNR and the ROC are plotted, respectively. For Fig. 7 the tests are designed such that the probability of false alarm is $P_{fa} \leq 10^{-6}$ and for Fig. 8 we have set SNR = 0 dB. It is seen from Fig. 7 that both the phase-array and the MIMO radars exhibit a diversity gain of 1, which verifies Theorem 4.
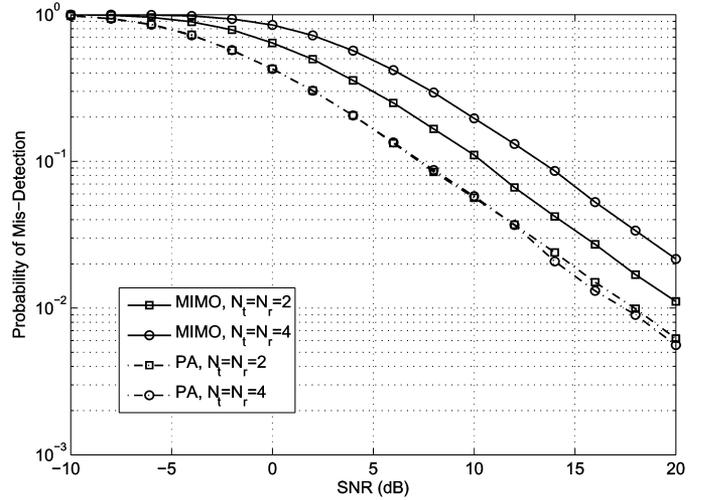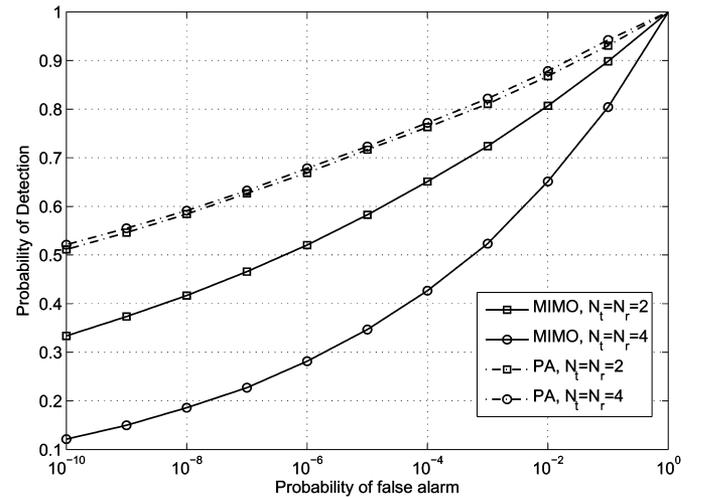
IX. CONCLUSION

In this paper, we have offered a framework for jointly detecting the presence of a target and estimating some unknown target parameters. We have provided a composite hypothesis test that satisfies some optimality criteria for both target detection and parameter estimation. By using this framework, we have proposed a new MIMO radar model for detecting the presence of a target in an unknown location and formulated a composite hypothesis test for solving this problem. In this problem, the unknown parameter of interest to be jointly estimated along with target detection, is the vector of time-delays that a transmitted waveform experiences from being emitted by the transmit antennas until being received by the receive antennas. For the proposed detection scheme, we also have analyzed the decay rate of the probability of mis-detection with increasing SNR while the false alarm probability is kept below a certain level (diversity gain). Our simulation results demonstrate that for the specific problem of joint target detection and time-delay estimation, deploying MIMO radars is advantageous for extended targets. On

the other hand, for point targets, the accuracies of target detection and time-delay estimation by conventional phased-array are comparable with those yielded by MIMO radars.

APPENDIX

Proof of Theorem 2: The pdf of the vector of received signals $\boldsymbol{R}$ for any given $\boldsymbol{\tau}$ and $\boldsymbol{h}$ is given by (30), shown at the bottom of the page. By taking into account the orthogonality assumption $\sum_{k=1}^{K} s_m[k; \tau_{m,n}] s_{m'}^*[k; \tau_{m',n}] = (\delta(m-m')/T_s)$, we can further simplify the term $D_1(\boldsymbol{\tau}, \boldsymbol{h})$ defined in (30) as follows:

$$
\begin{aligned}
D_1(\boldsymbol{\tau}, \boldsymbol{h}) &= \sum_{n=1}^{N_r} \sum_{k=1}^{K} \left| r_n[k] - \sqrt{\frac{E}{N_t}} c^{-\beta} \right. \\
&\quad \left. \cdot \sum_{m=1}^{N_t} \frac{1}{\tau_{m,n}^\beta} h_{m,n} s_m[k; \tau_{m,n}] \right|^2 \\
&= \sum_{k=1}^{K} \|\boldsymbol{r}[k]\|^2 + \frac{E}{N_t} c^{-2\beta} \\
&\quad \cdot \sum_{n=1}^{N_r} \sum_{m=1}^{N_t} \sum_{m'=1}^{N_t} \frac{1}{\tau_{m,n}^\beta \tau_{m',n}^\beta} h_{m,n} h_{m',n}^* \\
&\quad \cdot \underbrace{\sum_{k=1}^{K} s_m[k; \tau_{m,n}] s_{m'}^*[k; \tau_{m',n}]}_{(1/T_s)\delta(m-m')} \\
&\quad - \sqrt{\frac{E}{N_t}} c^{-\beta} \sum_{n=1}^{N_r} \sum_{m=1}^{N_t} h_{m,n} \frac{1}{\tau_{m,n}^\beta} \sum_{k=1}^{K} r_n^*[k] s_m[k; \tau_{m,n}] \\
&\quad - \sqrt{\frac{E}{N_t}} c^{-\beta} \sum_{n=1}^{N_r} \sum_{m=1}^{N_t} h_{m,n}^* \frac{1}{\tau_{m,n}^\beta} \sum_{k=1}^{K} r_n[k] s_m^*[k; \tau_{m,n}] \\
&= \sum_{k=1}^{K} \|\boldsymbol{r}[k]\|^2 + \frac{E}{T_s N_t} c^{-2\beta} \sum_{n=1}^{N_r} \sum_{m=1}^{N_t} \frac{1}{\tau_{m,n}^{2\beta}} |h_{m,n}|^2 \\
&\quad - \sum_{n=1}^{N_r} \sum_{m=1}^{N_t} h_{m,n} \underbrace{\sqrt{\frac{E}{N_t}} \frac{c^{-\beta}}{\tau_{m,n}^\beta} \sum_{k=1}^{K} r_n^*[k] s_m[k; \tau_{m,n}]}_{\triangleq a_{m,n}^*(\tau_{m,n})} \\
&\quad - \sum_{n=1}^{N_r} \sum_{m=1}^{N_t} h_{m,n}^* \underbrace{\sqrt{\frac{E}{N_t}} \frac{c^{-\beta}}{\tau_{m,n}^\beta} \sum_{k=1}^{K} r_n[k] s_m^*[k; \tau_{m,n}]}_{a_{m,n}(\tau_{m,n})}.
\end{aligned}
$$
(31)

For any given time-delay vector $\boldsymbol{\tau}$, define

$$
\boldsymbol{A}_{\boldsymbol{\tau}} \triangleq \frac{E}{T_s N_t} c^{-2\beta} \operatorname{diag}(\tau_{1,1}^{-2\beta}, \tau_{1,2}^{-2\beta}, \ldots, \tau_{N_t,N_r}^{-2\beta})
$$

and $\boldsymbol{a}_{\boldsymbol{\tau}} \triangleq [a_{1,1}(\tau_{1,1}), a_{1,2}(\tau_{1,2}), \ldots, a_{N_t,N_r}(\tau_{N_t,N_r})]^T$.
(32)

Then, $D_1(\boldsymbol{\tau}, \boldsymbol{h})$ can be represented in the matrix form as

$$
D_1(\boldsymbol{\tau}, \boldsymbol{h}) = \sum_{k=1}^{K} \|\boldsymbol{r}[k]\|^2 + \boldsymbol{h}^H \boldsymbol{A}_{\boldsymbol{\tau}} \boldsymbol{h} - \boldsymbol{h}^H \boldsymbol{a}_{\boldsymbol{\tau}} - \boldsymbol{a}_{\boldsymbol{\tau}}^H \boldsymbol{h}. \quad (33)
$$

By noting that the pdf of $\boldsymbol{h}$ is given by $f_{\boldsymbol{h}}(\boldsymbol{h}) = (\pi)^{-N_t N_r} \exp(-\|\boldsymbol{h}\|^2)$, we find the estimates of $\boldsymbol{\tau}$ as follows.

1) For finding $\hat{\boldsymbol{\tau}}^{\text{MAP}}$ by denoting the MAP estimate of $\boldsymbol{h}$ by $\hat{\boldsymbol{h}}$, setting $\boldsymbol{x} = [\hat{\boldsymbol{\tau}}^{\text{MAP}}, \hat{\boldsymbol{h}}]$, and considering the independence of $\boldsymbol{\tau}$ and $\boldsymbol{h}$, from (10) we get

$$
\begin{aligned}
[\hat{\boldsymbol{\tau}}^{\text{MAP}}; \hat{\boldsymbol{h}}] &= \arg \max_{\boldsymbol{\tau} \in \mathcal{A}(\mathcal{X}), \boldsymbol{h}} f_1(\boldsymbol{R}|\boldsymbol{\tau}, \boldsymbol{h}) f_{\boldsymbol{h}}(\boldsymbol{h}) \\
&= \arg \max_{\boldsymbol{\tau} \in \mathcal{A}(\mathcal{X})} \arg \max_{\boldsymbol{h}} f_1(\boldsymbol{R}|\boldsymbol{\tau}, \boldsymbol{h}) f_{\boldsymbol{h}}(\boldsymbol{h})
\end{aligned}
$$

or equivalently

$$
\hat{\boldsymbol{h}} = \arg \max_{\boldsymbol{h}} f_1(\boldsymbol{R}|\boldsymbol{\tau}, \boldsymbol{h}) f_{\boldsymbol{h}}(\boldsymbol{h}),
$$

$$
\text{and } \hat{\boldsymbol{\tau}}^{\text{MAP}} = \arg \max_{\boldsymbol{\tau} \in \mathcal{A}(\mathcal{X})} f_1(\boldsymbol{R}|\boldsymbol{\tau}, \hat{\boldsymbol{h}}) f_{\boldsymbol{h}}(\hat{\boldsymbol{h}}). \quad (34)
$$

Using (30), (33) and (34) and noting the definition of $\boldsymbol{a}_{\boldsymbol{\tau}}$ given in (32) provides that

$$
\begin{aligned}
\hat{\boldsymbol{h}} &= \arg \max_{\boldsymbol{h}} f_1(\boldsymbol{R}|\boldsymbol{\tau}, \boldsymbol{h}) f_{\boldsymbol{h}}(\boldsymbol{h}) \\
&= \arg \max_{\boldsymbol{h}} (\pi)^{-N_t N_r + K N_r} \\
&\quad \cdot \exp\left(-\left(\sum_k \|\boldsymbol{r}[k]\|^2 + \boldsymbol{h}^H \boldsymbol{A}_{\boldsymbol{\tau}} \boldsymbol{h} \right.\right. \\
&\qquad \left.\left. - \boldsymbol{h}^H \boldsymbol{a}_{\boldsymbol{\tau}} - \boldsymbol{a}_{\boldsymbol{\tau}}^H \boldsymbol{h} + \|\boldsymbol{h}\|^2\right)\right) \\
&= \arg \min_{\boldsymbol{h}} \left\{ \boldsymbol{h}^H \underbrace{(\boldsymbol{A}_{\boldsymbol{\tau}} + \boldsymbol{I}_{N_t N_r})}_{\triangleq \boldsymbol{B}_{\boldsymbol{\tau}}} \boldsymbol{h} - \boldsymbol{h}^H \boldsymbol{a}_{\boldsymbol{\tau}} - \boldsymbol{a}_{\boldsymbol{\tau}}^H \boldsymbol{h} \right\} \\
&= \boldsymbol{B}_{\boldsymbol{\tau}}^{-1} \boldsymbol{a}_{\boldsymbol{\tau}}.
\end{aligned}
$$
(35)

$$
f_1(\boldsymbol{R}|\boldsymbol{\tau}, \boldsymbol{h}) = (\pi)^{-K N_r} \exp\left(-\underbrace{\sum_{n=1}^{N_r} \sum_{k=1}^{K} \left| r_n[k] - \sqrt{\frac{E}{N_t}} c^{-\beta} \sum_{m=1}^{N_t} \frac{1}{\tau_{m,n}^\beta} h_{m,n} s_m[k; \tau_{m,n}] \right|^2}_{\triangleq D_1(\boldsymbol{\tau}, \boldsymbol{h})} \right). \quad (30)
$$

Based on the above estimate of $\boldsymbol{\tau}$, $D_1(\boldsymbol{\tau}, \hat{\boldsymbol{h}})$ given in (33) becomes

$$D_1(\boldsymbol{\tau}, \hat{\boldsymbol{h}}) = \sum_{k=1}^{K} \|\boldsymbol{r}[k]\|^2 - \boldsymbol{a}_{\boldsymbol{\tau}}^H \boldsymbol{B}_{\boldsymbol{\tau}}^{-1} \boldsymbol{a}_{\boldsymbol{\tau}} - \|\hat{\boldsymbol{h}}\|^2. \tag{36}$$

Hence, the ML estimate of $\boldsymbol{\tau}$ can be found by solving

$$
\begin{aligned}
\hat{\boldsymbol{\tau}}^{\mathrm{MAP}} &= \arg \max_{\boldsymbol{\tau} \in \mathcal{A}(\mathcal{X})} \log f_1(\boldsymbol{R}|\boldsymbol{\tau}, \hat{\boldsymbol{h}}) f_{\boldsymbol{h}}(\hat{\boldsymbol{h}}) \\
&= \arg \max_{\boldsymbol{\tau} \in \mathcal{A}(\mathcal{X})} \left\{ -D_1(\boldsymbol{\tau}, \hat{\boldsymbol{h}}) - \|\hat{\boldsymbol{h}}\|^2 \right\} \\
&= \arg \max_{\boldsymbol{\tau} \in \mathcal{A}(\mathcal{X})} \left\{ \boldsymbol{a}_{\boldsymbol{\tau}}^H \boldsymbol{B}_{\boldsymbol{\tau}}^{-1} \boldsymbol{a}_{\boldsymbol{\tau}} \right\} \\
&= \arg \max_{\boldsymbol{\tau} \in \mathcal{A}(\mathcal{X})} \left\{ \boldsymbol{a}_{\boldsymbol{\tau}}^H (\boldsymbol{A}_{\boldsymbol{\tau}} + \boldsymbol{I})^{-1} \boldsymbol{a}_{\boldsymbol{\tau}} \right\} \\
&= \arg \max_{\boldsymbol{\tau} \in \mathcal{A}(\mathcal{X})} \left\{ \sum_{m=1}^{N_t} \sum_{n=1}^{N_r} \frac{|a_{m,n}(\tau_{m,n})|^2}{\frac{E}{T_s N_t} (c\tau_{m,n})^{-2\beta} + 1} \right\}
\end{aligned}
\tag{37}
$$
$$\tag{38}$$

which concludes the proof.

2) For this case which we average out the effect of $\boldsymbol{h}$ by setting $\boldsymbol{x} = \boldsymbol{\tau}$ from (10) we get (39)–(41), shown at the bottom of the page. Noting the definition of $a_{m,n}(\tau_{m,n})$ given in (31) concludes the proof.

Proof of Theorem 3: In order to find the ML estimate of $\boldsymbol{\tau}$ and ζ form (10) we have

$$
\begin{aligned}
[\boldsymbol{\tau}, \zeta] &= \arg \max_{\boldsymbol{\tau} \in \mathcal{A}(\mathcal{X}), \zeta} f_1(\boldsymbol{R}|\boldsymbol{\tau}, \zeta) \\
&= \arg \max_{\boldsymbol{\tau} \in \mathcal{A}(\mathcal{X})} \arg \max_{\zeta} f_1(\boldsymbol{R}|\boldsymbol{\tau}, \zeta)
\end{aligned}
$$

or equivalently

$$\hat{\zeta} = \arg \max_{\zeta} f_1(\boldsymbol{R}|\boldsymbol{\tau}, \zeta) \text{ and } \hat{\boldsymbol{\tau}} = \arg \max_{\boldsymbol{\tau} \in \mathcal{A}(\mathcal{X})} f_1(\boldsymbol{R}|\boldsymbol{\tau}, \hat{\tau}).$$

On the other hand, from (18) the likelihood $f_1(\boldsymbol{R} \mid \boldsymbol{\tau}, \hat{\tau})$ is given by (42), shown at the bottom of the page. By taking into account the orthonormality assumption on $s_m[k; \tau_{m,n}]$ we get

$$D_2(\boldsymbol{\tau}, \zeta) = \sum_{n=1}^{N_r} \sum_{k=1}^{K} \left| r_n[k] - \sqrt{\frac{E}{N_t}} \zeta c^{-\beta} \right.$$

$$
\begin{aligned}
\hat{\boldsymbol{\tau}}^{\mathrm{ave}} &= \arg \max_{\boldsymbol{\tau} \in \mathcal{A}(\mathcal{X})} f_1(\boldsymbol{R}|\boldsymbol{\tau}) = \arg \max_{\boldsymbol{\tau} \in \mathcal{A}(\mathcal{X})} \int_{\boldsymbol{h}} f_1(\boldsymbol{R}|\boldsymbol{\tau}, \boldsymbol{h}) f_{\boldsymbol{h}}(\boldsymbol{h}) d\boldsymbol{h} \\
&= \arg \max_{\boldsymbol{\tau} \in \mathcal{A}(\mathcal{X})} \int_{\boldsymbol{h}} \exp\left(-D_1(\boldsymbol{\tau}, \boldsymbol{h})\right) f_{\boldsymbol{h}}(\boldsymbol{h}) d\boldsymbol{h} \\
&= \arg \max_{\boldsymbol{\tau} \in \mathcal{A}(\mathcal{X})} \int_{\boldsymbol{h}} \exp\left(-\left(\boldsymbol{h}^H \underbrace{(\boldsymbol{A}_{\boldsymbol{\tau}} + \boldsymbol{I}_{N_t N_r})}_{\triangleq \boldsymbol{B}_{\boldsymbol{\tau}}} \boldsymbol{h} - \boldsymbol{h}^H \boldsymbol{a}_{\boldsymbol{\tau}} - \boldsymbol{a}_{\boldsymbol{\tau}}^H \boldsymbol{h} \right) \right) d\boldsymbol{h} \\
&= \arg \max_{\boldsymbol{\tau} \in \mathcal{A}(\mathcal{X})} \int_{\boldsymbol{h}} \exp\left(-\left\{ (\boldsymbol{h} - \boldsymbol{B}_{\boldsymbol{\tau}}^{-1} \boldsymbol{a}_{\boldsymbol{\tau}})^H \boldsymbol{B}_{\boldsymbol{\tau}} (\boldsymbol{h} - \boldsymbol{B}_{\boldsymbol{\tau}}^{-1} \boldsymbol{a}_{\boldsymbol{\tau}}) - \boldsymbol{a}_{\boldsymbol{\tau}}^H \boldsymbol{B}_{\boldsymbol{\tau}}^{-1} \boldsymbol{a}_{\boldsymbol{\tau}} \right\} \right) d\boldsymbol{h} \\
&= \arg \max_{\boldsymbol{\tau} \in \mathcal{A}(\mathcal{X})} \exp\left(\boldsymbol{a}_{\boldsymbol{\tau}}^H \boldsymbol{B}_{\boldsymbol{\tau}}^{-1} \boldsymbol{a}_{\boldsymbol{\tau}} \right) \int_{\boldsymbol{h}} \exp\left(-\left\{ (\boldsymbol{h} - \boldsymbol{B}_{\boldsymbol{\tau}}^{-1} \boldsymbol{a}_{\boldsymbol{\tau}})^H \boldsymbol{B}_{\boldsymbol{\tau}} (\boldsymbol{h} - \boldsymbol{B}_{\boldsymbol{\tau}}^{-1} \boldsymbol{a}_{\boldsymbol{\tau}}) \right\} \right) d\boldsymbol{h} \\
&= \arg \max_{\boldsymbol{\tau} \in \mathcal{A}} \exp\left(\boldsymbol{a}_{\boldsymbol{\tau}}^H \boldsymbol{B}_{\boldsymbol{\tau}}^{-1} \boldsymbol{a}_{\boldsymbol{\tau}} \right) |\boldsymbol{B}_{\boldsymbol{\tau}}|^{-1} \\
&= \arg \max_{\boldsymbol{\tau} \in \mathcal{A}(\mathcal{X})} \left\{ \boldsymbol{a}_{\boldsymbol{\tau}}^H \boldsymbol{B}_{\boldsymbol{\tau}}^{-1} \boldsymbol{a}_{\boldsymbol{\tau}} - \log |\boldsymbol{B}_{\boldsymbol{\tau}}| \right\} \\
&= \arg \max_{\boldsymbol{\tau} \in \mathcal{A}(\mathcal{X})} \left\{ \boldsymbol{a}_{\boldsymbol{\tau}}^H (\boldsymbol{A}_{\boldsymbol{\tau}} + \boldsymbol{I})^{-1} \boldsymbol{a}_{\boldsymbol{\tau}} - \log |\boldsymbol{A}_{\boldsymbol{\tau}} + \boldsymbol{I}| \right\} \\
&= \arg \max_{\boldsymbol{\tau} \in \mathcal{A}(\mathcal{X})} \sum_{m=1}^{N_t} \sum_{n=1}^{N_r} \left\{ \frac{|a_{m,n}(\tau_{m,n})|^2}{\frac{E}{T_s N_t} (c\tau_{m,n})^{-2\beta} + 1} - \log\left(\frac{E}{T_s N_t} (c\tau_{m,n})^{-2\beta} + 1 \right) \right\}.
\end{aligned}
$$

$$\tag{39}$$
$$\tag{40}$$
$$\tag{41}$$

$$f_1(\boldsymbol{R}|\boldsymbol{\tau}, \zeta) = (\pi)^{-K N_r} \exp\left(-\underbrace{\sum_{n=1}^{N_r} \sum_{k=1}^{K} \left| r_n[k] - \sqrt{\frac{E}{N_t}} \zeta c^{-\beta} \sum_{m=1}^{N_t} \frac{e^{-j2\pi f_c \tau_{m,n}}}{\tau_{m,n}^{\beta}} s_m[k; \tau_{m,n}] \right|^2}_{\triangleq D_2(\boldsymbol{\tau}, \zeta)} \right). \tag{42}$$

$$
\cdot \sum_{m=1}^{N_t} \frac{e^{-j2\pi f_c \tau_{m,n}}}{\tau_{m,n}^\beta} s_m[k;\tau_{m,n}] \Bigg|^2
$$

$$
= \sum_{k=1}^{K} \|\boldsymbol{r}[k]\|^2 + \frac{E}{T_s N_t} |\zeta|^2 c^{-2\beta} \sum_{n=1}^{N_r}
$$

$$
\cdot \sum_{m=1}^{N_t} \frac{1}{(c\tau_{m,n})^{2\beta}}
$$

$$
- \sum_{n=1}^{N_r} \sum_{m=1}^{N_t} e^{-j2\pi f_c \tau_{m,n}} \sqrt{\frac{E}{N_t}} \zeta \frac{c^{-\beta}}{\tau_{m,n}^\beta}
$$

$$
\cdot \sum_{k=1}^{K} r_n^*[k] s_m[k;\tau_{m,n}]
$$

$$
- \sum_{n=1}^{N_r} \sum_{m=1}^{N_t} e^{j2\pi f_c \tau_{m,n}} \sqrt{\frac{E}{N_t}} \zeta^* \frac{c^{-\beta}}{\tau_{m,n}^\beta}
$$

$$
\cdot \sum_{k=1}^{K} r_n[k] s_m^*[k;\tau_{m,n}]. \tag{43}
$$

$D_2(\boldsymbol{\tau},\zeta)$ is quadratic in ζ and its minimum which is attained at the ML estimate of ζ is given by

$$
\hat{\zeta} = \arg\max_\zeta \log f_1(\boldsymbol{R}|\boldsymbol{\tau},\zeta) = \arg\min_\zeta D_2(\boldsymbol{\tau},\zeta)
$$

$$
= \frac{\sum_{m=1}^{N_t} \sum_{n=1}^{N_r} \frac{1}{(c\tau_{m,n})^\beta} e^{j2\pi f_c \tau_{m,n}} \sum_{k=1}^{K} r_n[k] s_m^*[k;\tau_{m,n}]}{\frac{1}{T_s} \sqrt{\frac{E}{N_T}} \sum_{m=1}^{N_t} \sum_{n=1}^{N_r} \frac{1}{(c\tau_{m,n})^{2\beta}}}.
$$

$$
\tag{44}
$$

By substituting (44) back in (43), and after some manipulation, $D_2(\boldsymbol{\tau},\hat{\zeta})$ becomes

$$
D_2(\boldsymbol{\tau},\hat{\zeta}) = \sum_{k=1}^{K} \|\boldsymbol{r}[k]\|^2 - \frac{E}{T_s N_t} |\hat{\zeta}|^2 \sum_{m=1}^{N_t} \sum_{n=1}^{N_r} \frac{1}{(c\tau_{m,n})^{2\beta}}.
$$

Therefore,

$$
\hat{\boldsymbol{\tau}} = \arg\max_{\boldsymbol{\tau}\in\mathcal{A}(\mathcal{X})} \log f_1(\boldsymbol{R}|\boldsymbol{\tau},\hat{\zeta})
$$

$$
= \arg\min_\zeta D_2(\boldsymbol{\tau},\hat{\zeta})
$$

$$
= \arg\max_{\boldsymbol{\tau}\in\mathcal{A}(\mathcal{X})} \left\{ |\hat{\zeta}|^2 \sum_{m=1}^{N_t} \sum_{n=1}^{N_r} \frac{1}{(c\tau_{m,n})^{2\beta}} \right\}
$$

$$
= \arg\max_{\boldsymbol{\tau}\in\mathcal{A}(\mathcal{X})} \frac{\left| \sum_{m=1}^{N_t} \sum_{n=1}^{N_r} \frac{e^{j2\pi f_c \tau_{m,n}}}{\tau_{m,n}^\beta} \sum_{k=1}^{K} r_n[k] s_m^*[k;\tau_{m,n}] \right|^2}{\sum_{m=1}^{N_t} \sum_{n=1}^{N_r} \frac{1}{\tau_{m,n}^{2\beta}}}.
$$

$$
\tag{45}
$$

Proof of Lemma 3: We provide the proof by induction.
1) $N = 2$. We define

$$
q(t_1, t_2) \triangleq \left| e^{j\alpha t_1} g_1(t_1) + e^{j\alpha t_2} g_2(t_1) \right|.
$$

Then

$$
q^2(t_1, t_2) = |g_1(t_1)|^2 + |g_2(t_1)|^2 + e^{j\alpha(t_1-t_2)} g_1(t_1) g_2^*(t_1)
$$

$$
+ e^{j\alpha(t_2-t_1)} g_2(t_1) g_1^*(t_1)
$$

and therefore,

$$
\frac{\partial(q^2(t_1,t_2))}{\partial t_2} = j\alpha \Big[e^{j\alpha(t_2-t_1)} g_2(t_1) g_1^*(t_1)
$$

$$
- e^{j\alpha(t_1-t_2)} g_1(t_1) f_2^*(t_1) \Big].
$$

For finding $\max_{t_2} q(t_1, t_2)$ we set $(\partial(q^2(t_1,t_2))/\partial t_2) = 0$ and obtain

$$
e^{j\alpha\hat{t}_2} = e^{j\alpha t_1} \sqrt{\frac{g_1(t_1) g_2^*(t_1)}{g_1^*(t_1) g_2(t_1)}}.
$$

We can check that this is a maximum by noting that

$$
\frac{\partial^2(q^2(t_1,t_2))}{\partial t_2^2} \Bigg|_{t_2=\hat{t}_2} = (j\alpha)^2 \Big[e^{j\alpha(\hat{t}_2-t_1)} g_1^*(t_1) g_2(t_1)
$$

$$
+ e^{j\alpha(t_1-\hat{t}_2)} g_1(t_1) g_2^*(t_1) \Big]
$$

$$
= -2(\alpha)^2 |g_1(t_1) g_2(t_1)| < 0.
$$

Hence,

$$
\max_{t_2} q(t_1, t_2) = q(t_1, \hat{t}_2)
$$

$$
= \sqrt{|g_1(t_1)|^2 + |g_2(t_1)|^2 + 2|g_1(t_1) g_2(t_1)|}
$$

$$
= \sum_{i=1}^{2} |g_i(t_1)|.
$$

2) Inductive assumption

$$
\max_{\{t_2,\dots,t_N\}} \left| \sum_{i=1}^{N} e^{j\alpha t_i} g_i(t_1) \right| = \sum_{i=1}^{N} |g_i(t_1)|.
$$

3) Claim

$$
\max_{\{t_2,\dots,t_{N+1}\}} \left| \sum_{i=1}^{N+1} e^{j\alpha t_i} g_i(t_1) \right| = \sum_{i=1}^{N+1} |g_i(t_1)|.
$$

Let $\boldsymbol{t} \triangleq [t_1 \dots t_{N+1}]$ and $q(\boldsymbol{t}) \triangleq \left| \sum_{i=1}^{N+1} e^{j\alpha t_i} g_i(t_1) \right|$, then

$$
\frac{\partial(q^2(\boldsymbol{t}))}{\partial t_{N+1}} = \frac{\partial}{\partial t_{N+1}} \Bigg[\sum_{i=1}^{N} e^{j\alpha(t_{N+1}-t_i)} g_i^*(t_1) g_{N+1}(t_1)
$$

$$
+ \sum_{i=1}^{N} e^{j\alpha(t_i-t_{N+1})} g_i(t_1) g_{N+1}^*(t_1) \Bigg]
$$

$$
= j\alpha \Bigg[\sum_{i=1}^{N} e^{j\alpha(t_{n+1}-t_i)} g_i^*(t_1) g_{N+1}(t_1)
$$

$$
+ \sum_{i=1}^{N} e^{j\alpha(t_i-t_{N+1})} g_i(t_1) g_{N+1}^*(t_1) \Bigg].
$$

If we set $(\partial(q^2(\boldsymbol{t}))/\partial t_{n+1}) = 0$, then

$$e^{2j\alpha\hat{t}_{N+1}} = \frac{\sum_{i=1}^{N} e^{j\alpha t_i} g_i(t_1)}{\sum_{i=1}^{N} e^{-j\alpha t_i} g_i^*(t_1)} \frac{g_{N+1}^*(t_1)}{g_{N+1}(t_1)}.$$

Also $\hat{t}_{N+1}$ is a maximum since

$$\left. \frac{\partial^2(q^2(\boldsymbol{t}))}{\partial t_{N+1}^2} \right|_{t_{N+1}=\hat{t}_{N+1}}$$

$$= (j\alpha)^2 \left[\sum_{i=1}^{N} e^{j\alpha(\hat{t}_{N+1}-t_i)} g_i^*(t_1) g_{N+1}(t_1) \right.$$

$$\left. + \sum_{i=1}^{N} e^{j\alpha(t_i-\hat{t}_{N+1})} g_i(t_1) g_{N+1}^*(t_1) \right]$$

$$= (j\alpha)^2 \left[2 \left(\sum_{i=1}^{N} e^{j\alpha t_i} g_i(t_1) g_{N+1}^*(t_1) \right. \right.$$

$$\left. \left. \cdot \sum_{k=1}^{N} e^{-j\alpha t_k} g_k^*(t_1) g_{N+1}(t_1) \right)^{(1/2)} \right]$$

$$= -2\alpha^2 \left| \sum_{i=1}^{N} e^{j\alpha t_i} g_i(t_1) g_{N+1}^*(t_1) \right| < 0.$$

Therefore, by substituting $\hat{t}_{N+1}$ and some simple manipulations we get

$$\max_{t_{N+1}} q^2(\boldsymbol{t}) = q^2(t_1,\ldots,t_N,\hat{t}_{N+1})$$

$$= \left| \sum_{i=1}^{N} e^{j\alpha t_i} g_i(t_1) \right|^2 + |g_{N+1}(t_1)|^2$$

$$+ 2 \left(\sum_{i=1}^{N} e^{j\alpha t_i} g_i(t_1) g_{N+1}^*(t_1) \right.$$

$$\left. \cdot \sum_{k=1}^{N} e^{-j\alpha t_k} g_k^*(t_1) g_{N+1}(t_1) \right)^{(1/2)}$$

$$= \left| \sum_{i=1}^{N} e^{j\alpha t_i} g_i(t_1) \right|^2 + |g_{N+1}(t_1)|^2$$

$$+ 2 \left| \sum_{i=1}^{N} e^{j\alpha t_i} g_i(t_1) g_{N+1}^*(t_1) \right|$$

$$= \left| \sum_{i=1}^{N} e^{j\alpha t_i} g_i(t_1) \right|^2 + |g_{N+1}(t_1)|^2$$

$$+ 2 |g_{N+1}(t_1)| \left| \sum_{i=1}^{N} e^{j\alpha t_i} g_i(t_1) \right|$$

$$= \left(\left| \sum_{i=1}^{N} e^{j\alpha t_i} g_i(t_1) \right| + |g_{N+1}(t_1)| \right)^2.$$

As a result

$$\max_{\{t_2,\ldots,t_{N+1}\}} q(\boldsymbol{t})$$

$$= \max_{\{t_2,\ldots,t_N\}} \max_{t_{N+1}} q(\boldsymbol{t})$$

$$= \max_{\{t_2,\ldots,t_N\}} \left\{ \left| \sum_{i=1}^{N} e^{j\alpha t_i} g_i(t_1) \right| \right\} + |g_{N+1}(t_1)|$$

$$= \sum_{i=1}^{N} |g_i(t_1)| + |g_{N+1}(t_1)| = \sum_{i=1}^{N+1} |g_i(t_1)|.$$

Proof of Lemma 4:

1) By recalling the definition of $S_n(\boldsymbol{\tau}) = \sum_{m=1}^{N_t} (1/(c\tau_{m,n})^\beta)\hat{s}_m e^{j2\pi f_c(\tau_{1,1}-\tau_{m,n})}$ and the pdf of h given by $f_h(h) = (1/\sqrt{\pi})e^{-|h|^2}$, the likelihood under hypothesis $\mathcal{H}_1$ is given by

$$f_1(\boldsymbol{R}|\boldsymbol{\tau},h) = (\pi)^{-KN_r}$$

$$\cdot \exp\left(-\underbrace{\sum_{n=1}^{N_r}\sum_{k=1}^{K}\left| r_n[k] - \sqrt{\frac{E}{N_t}}S_n(\boldsymbol{\tau})hs[k;\tau_{1,1}] \right|^2}_{\triangleq D_2(\boldsymbol{\tau},h)} \right).$$

We further simplify $D_3(\boldsymbol{\tau},h)$ as follows:

$$D_2(\boldsymbol{\tau},h) = \sum_{n=1}^{N_r}\sum_{k=1}^{K}\left| r_n[k] - \sqrt{\frac{E}{N_t}}S_n(\boldsymbol{\tau})hs[k;\tau_{1,1}] \right|^2$$

$$= \sum_{k=1}^{K} \|\boldsymbol{r}[k]\|^2 + |h|^2 \left\{ \frac{E}{T_sN_t}\sum_{n=1}^{N_r}|S_n(\boldsymbol{\tau})|^2 \right\}$$

$$- h^*\sqrt{\frac{E}{N_t}}\sum_{n=1}^{N_r}S_n^*(\boldsymbol{\tau})\sum_{k=1}^{K}r_n[k]s^*[k;\tau_{1,1}]$$

$$- h\sqrt{\frac{E}{N_t}}\sum_{n=1}^{N_r}S_n(\boldsymbol{\tau})\sum_{k=1}^{K}r_n^*[k]s[k;\tau_{1,1}].$$

Therefore, the MAP estimate of h is given by

$$\hat{h} = \arg\max_h \{f_1(\boldsymbol{R}|\boldsymbol{\tau},h)f_h(h)\}$$

$$= \arg\min_h \left\{ \hat{D}_2(\boldsymbol{\tau},h) + |h|^2 \right\}$$

$$= \frac{\sqrt{\frac{E}{N_t}}\sum_{n=1}^{N_r}S_n^*(\boldsymbol{\tau})\sum_{k=1}^{K}r_n[k]s^*[k;\tau_{1,1}]}{\frac{E}{T_sN_t}\sum_{n=1}^{N_r}|S_n(\boldsymbol{\tau})|^2 + 1} \qquad (46)$$

which in turn after some manipulations provides that

$$\hat{D}_2(\boldsymbol{\tau},\hat{h}) + |\hat{h}|^2 = \sum_{k=1}^{K}\|\boldsymbol{r}[k]\|^2 - |\hat{h}|^2\left\{ \frac{E}{T_sN_t}\sum_{n=1}^{N_r}|S_n(\boldsymbol{\tau})|^2 \right\}.$$

Therefore,

$$\hat{\boldsymbol{\tau}}^{\text{MAP}} = \arg\max_{\boldsymbol{\tau}\in\mathcal{A}'(\mathcal{X}')} \left\{ f_1(\boldsymbol{R}|\boldsymbol{\tau},\hat{h})f_h(\hat{h}) \right\}$$

$$
= \arg \max_{\boldsymbol{\tau} \in \mathcal{A}'(\mathcal{X}')} |\hat{h}|^2 \left\{ \frac{E}{T_s N_t} \sum_{n=1}^{N_r} |S_n(\boldsymbol{\tau})|^2 + 1 \right\}
$$

$$
= \arg \max_{\boldsymbol{\tau} \in \mathcal{A}'(\mathcal{X}')} \frac{\left| \sum_{n=1}^{N_r} S_n^*(\boldsymbol{\tau}) \sum_{k=1}^{K} r_n[k] s^*[k; \tau_{1,1}] \right|^2}{\frac{1}{T_s} \sum_{n=1}^{N_r} |S_n(\boldsymbol{\tau})|^2 + \frac{N_t}{E}}
$$

(47)

which is the desired result.

2) By recalling the definition of $S_n(\boldsymbol{\tau}) = \sum_{m=1}^{N_t} (1/(c\tau_{m,n})^\beta) \hat{s}_m e^{j2\pi f_c(\tau_{1,1} - \tau_{m,n})}$ and the pdf of h given by $f_h(h) = (1/\sqrt{\pi}) e^{-|h|^2}$, the likelihood under hypothesis $\mathcal{H}_1$ is given by the equation, shown at the bottom of the page. We further simplify $D_3(\boldsymbol{\tau}, \zeta)$ as follows:

$$
\begin{aligned}
&D_3(\boldsymbol{\tau}, \zeta) \\
&= \sum_{n=1}^{N_r} \sum_{k=1}^{K} \left| r_n[k] - \sqrt{\frac{E}{N_t}} S_n(\boldsymbol{\tau}) h s[k; \tau_{1,1}] \right|^2 + |h|^2 \\
&= \sum_{k=1}^{K} \|\boldsymbol{r}[k]\|^2 + |h|^2 \left\{ \frac{E}{T_s N_t} \sum_{n=1}^{N_r} |S_n(\boldsymbol{\tau})|^2 + 1 \right\} \\
&\quad - h^* \sqrt{\frac{E}{N_t}} \sum_{n=1}^{N_r} S_n^*(\boldsymbol{\tau}) \sum_{k=1}^{K} r_n[k] s^*[k; \tau_{1,1}] \\
&\quad - h \sqrt{\frac{E}{N_t}} \sum_{n=1}^{N_r} S_n(\boldsymbol{\tau}) \sum_{k=1}^{K} r_n^*[k] s[k; \tau_{1,1}] \\
&= \sum_{k=1}^{K} \|\boldsymbol{r}[k]\|^2
\end{aligned}
$$

$$
+ \left| h \sqrt{\frac{E}{T_s \cdot N_t} \sum_{n=1}^{N_r} |S_n(\boldsymbol{\tau})|^2 + 1} \right.
$$

$$
\left. - \frac{\sqrt{\frac{E}{N_t}} \sum_{n=1}^{N_r} S_n^*(\boldsymbol{\tau}) \sum_{k=1}^{K} r_n[k] s^*[k; \tau_{1,1}]}{\sqrt{\frac{E}{T_s \cdot N_t} \sum_{n=1}^{N_r} |S_n(\boldsymbol{\tau})|^2 + 1}} \right|^2
$$

$$
- \frac{\frac{E}{N_t} \left| \sum_{n=1}^{N_r} S_n^*(\boldsymbol{\tau}) \sum_{k=1}^{K} r_n[k] s^*[k; \tau_{1,1}] \right|^2}{\frac{E}{T_s \cdot N_t} \sum_{n=1}^{N_r} |S_n(\boldsymbol{\tau})|^2 + 1}.
$$

(48)

By following the same line of argument as in the proof of Theorem 2, it can be readily demonstrated that the ML estimate of the time-delay for phased-array system is given by

$$
\begin{aligned}
&\hat{\boldsymbol{\tau}}^{\text{ave}} \\
&= \arg \max_{\boldsymbol{\tau} \in \mathcal{A}'(\mathcal{X}')} f_1(\boldsymbol{R}|\boldsymbol{\tau}) \\
&= \arg \max_{\boldsymbol{\tau} \in \mathcal{A}'(\mathcal{X}')} \left\{ \frac{\left| \sum_{n=1}^{N_r} S_n^*(\boldsymbol{\tau}) \sum_{k=1}^{K} r_n[k] s^*[k; \tau_{1,1}] \right|^2}{\frac{1}{T_s} \sum_{N=1}^{N_r} |S_n(\boldsymbol{\tau})|^2 + \frac{N_t}{E}} \right. \\
&\quad \left. - \frac{1}{2} \log \left(\frac{E}{T_s N_t} \sum_{n=1}^{N_r} |S_n(\boldsymbol{\tau})|^2 + 1 \right) \right\}.
\end{aligned}
$$

3) Setting $P = 1$ in (4), it is seen that $h_{m,n} = \zeta e^{-j2\pi f_c \tau_{m,n}}$. Therefore, the likelihood under hypothesis $\mathcal{H}_1$ becomes as shown in the equation at the bottom of the page. By defining $\hat{S}_n(\boldsymbol{\tau}) \triangleq \sum_{m=1}^{N_t} (1/(c\tau_{m,n})^\beta) \hat{s}_m e^{j2\pi f_c(\tau_{1,1} - 2\tau_{m,n})}$ and

---

$$
f_1(\boldsymbol{R}|\boldsymbol{\tau}) = \int_h f_1(\boldsymbol{R}|\boldsymbol{\tau}, h) f_h(h) dh
$$

$$
= \frac{(\pi)^{-KN_r}}{\sqrt{\pi}} \int_h \exp \left(-\underbrace{\sum_{n=1}^{N_r} \sum_{k=1}^{K} \left| r_n[k] - \sqrt{\frac{E}{N_t}} S_n(\boldsymbol{\tau}) h s[k; \tau_{1,1}] \right|^2 + |h|^2}_{\triangleq D_3(\boldsymbol{\tau})} \right) dh.
$$

$$
f_1(\boldsymbol{R}|\boldsymbol{\tau}, \zeta) = (\pi)^{-KN_r} \exp \left(-\underbrace{\sum_{n=1}^{N_r} \sum_{k=1}^{K} \left| r_n[k] - \zeta \sqrt{\frac{E}{N_t}} s[k; \tau_{1,1}] \sum_{m=1}^{N_t} \frac{1}{(c\tau_{m,n})^\beta} \hat{s}_m e^{j2\pi f_c(\tau_{1,1} - 2\tau_{m,n})} \right|^2}_{\triangleq D_4(\boldsymbol{\tau}, \zeta)} \right).
$$

following the same line of argument as in the previous part the ML estimate for ζ is found as

$$
\begin{aligned}
\hat{\zeta} &= \arg\max_{\zeta} \left\{ \log f_1(\boldsymbol{R}|\boldsymbol{\tau}, \zeta) \right\} \\
&= \arg\min_{\zeta} \left\{ D_4(\boldsymbol{\tau}, \zeta) \right\} = \frac{\sum_{n=1}^{N_r} \hat{S}_n^*(\boldsymbol{\tau}) \sum_{k=1}^{K} r_n[k]s^*[k;\tau_{1,1}]}{\frac{1}{T_s}\sqrt{\frac{E}{N_t}} \sum_{n=1}^{N_r} |\hat{S}_n(\boldsymbol{\tau})|^2}
\end{aligned}
$$

and consequently

$$
D_4(\boldsymbol{\tau}, \hat{\zeta}) = \sum_{k=1}^{K} \|\boldsymbol{r}[k]\|^2 - \frac{E}{T_s N_t}|\hat{\zeta}|^2 \sum_{n=1}^{N_r} |\hat{S}_n(\boldsymbol{\tau})|^2.
$$

Therefore, by following a similar approach as in part 1 we get

$$
\begin{aligned}
\hat{\boldsymbol{\tau}} &= \arg\max_{\boldsymbol{\tau} \in \mathcal{A}'(\mathcal{X}')} f_1(\boldsymbol{R}|\boldsymbol{\tau}, \hat{\zeta}) \\
&= \arg\max_{\boldsymbol{\tau} \in \mathcal{A}'} \left\{ \frac{E}{T_s N_t}|\hat{\zeta}|^2 \sum_{n=1}^{N_r} |\hat{S}_n(\boldsymbol{\tau})|^2 \right\} \\
&= \arg\max_{\boldsymbol{\tau} \in \mathcal{A}'(\mathcal{X}')} \frac{\left| \sum_{n=1}^{N_r} \hat{S}_n^*(\boldsymbol{\tau}) \sum_{k=1}^{K} r_n[k]s^*[k;\tau_{1,1}] \right|^2}{\frac{1}{T_s} \sum_{n=1}^{N_r} |\hat{S}_n(\boldsymbol{\tau})|^2}
\end{aligned} \tag{49}
$$

which is the desired result.

Proof of Lemma 6: We define the events

$$
\mathcal{D}_1 \triangleq \bigcup_{m=1}^{M} \left\{ Y_m^2 < \gamma \right\}, \text{ and } \mathcal{D}_2 \triangleq \left\{ \sum_{m=1}^{M} Y_m^2 < \gamma \right\},
$$

$$
\text{and } \mathcal{D}_3 \triangleq \bigcup_{m=1}^{M} \left\{ Y_m^2 < \frac{\gamma}{M} \right\}.
$$

Clearly as $\mathcal{D}_3 \subseteq \mathcal{D}_2 \subseteq \mathcal{D}_1$ we have $\Pr(\mathcal{D}_3) \leq \Pr(\mathcal{D}_2) \leq \Pr(\mathcal{D}_1)$, where $\Pr(\mathcal{D}_2)$ is the probability of interest in (21). In order to analyze $P(\mathcal{D}_1)$, we define random variables $\hat{Y}_m \sim \mathcal{N}\left(\rho \cdot |\mu_m|, \sigma^2\right)$, for which we have

$$
\begin{aligned}
\Pr\left(Y_m^2 < \gamma\right) &= \Pr\left(\hat{Y}_m^2 < \gamma\right) = \Pr\left(-\sqrt{\gamma} < \hat{Y}_m < \sqrt{\gamma}\right) \\
&= Q\left(\frac{\rho|\mu_m| - \sqrt{\gamma}}{\sigma}\right) - Q\left(\frac{\rho|\mu_m| + \sqrt{\gamma}}{\sigma}\right) \\
&\stackrel{\circ}{=} Q\left(\frac{\rho|\mu_m| - \sqrt{\gamma}}{\sigma}\right) \tag{50} \\
&\stackrel{\circ}{=} Q\left(\frac{\rho|\mu_m|}{\sigma}\right) \tag{51}
\end{aligned}
$$

where the transition in (50) holds by noting that for any choice of $\gamma > \sigma^2$, from the table of $Q(\cdot)$ function it is readily verified that for sufficiently large values of x, and any fixed value $\Delta > 0$, $Q(x) \gg Q(x - \Delta)$. The asymptotic equality in (51) is justified

by noting that $\rho|\mu_m| \gg \sqrt{\gamma}$. By further using the following known bounds on the $Q(\cdot)$:

$$
\forall \ x \in \mathbb{R}^+,
$$

$$
\frac{1}{\sqrt{2\pi}x}\underbrace{\left(1 - \frac{1}{x^2}\right)}_{\stackrel{\circ}{=}1}e^{-x^2/2} \leq Q(x) \leq \frac{1}{\sqrt{2\pi}x}e^{-x^2/2}
$$

we get

$$
\forall \ x \in \mathbb{R}^+,
$$

$$
\frac{1}{\sqrt{2\pi}x}e^{-x^2/2} \stackrel{\circ}{\leq} Q(x) \stackrel{\circ}{\leq} \frac{1}{\sqrt{2\pi}x}e^{-x^2/2}
$$

$$
\Rightarrow Q(x) \stackrel{\circ}{=} \frac{1}{\sqrt{2\pi}x}e^{-x^2/2}.
$$

By further taking into account that $\left(1/\sqrt{2\pi}x\right)e^{-x^2/2} \doteq e^{-x^2/2}$ and noting Remark 1 we get

$$
Q(x) \doteq e^{-x^2/2}. \tag{52}
$$

Invoking the exponential equivalence in (52) on (51) provides

$$
\Pr\left(Y_m^2 < \gamma\right) \doteq e^{-\left(\rho^2 \mu_m^2/2\sigma^2\right)}. \tag{53}
$$

As μ_m is an unknown random variable distributed as $\mathcal{N}\left(0, \sigma_\mu^2\right)$, by averaging out its effect we get

$$
\begin{aligned}
&\mathbb{E}_{\mu_m}\left[\Pr\left(Y_m^2 < \gamma\right)\right] \\
&\doteq \frac{1}{\sqrt{2\pi}} \int_{-\infty}^{\infty} e^{-\left(\left(\rho^2/\sigma^2\right) + \left(1/\sigma_m^2\right)\right)\left(\mu_m^2/2\right)} d\mu_m \\
&= \frac{1}{\sqrt{\frac{\rho^2}{\sigma^2} + \frac{1}{\sigma_m^2}}} \doteq \rho^{-1}. \tag{54}
\end{aligned}
$$

Next, by considering the statistical independence of $\{Y_m\}_{m=1}^{M}$ we consequently find

$$
\mathbb{E}_{\boldsymbol{\mu}}\left[\Pr(\mathcal{D}_1)\right] = \prod_{m=1}^{M} \mathbb{E}_{\mu_m}\left[\Pr(Y_m^2 < \gamma)\right] \doteq \rho^{-M}. \tag{55}
$$

Note that, as long as the asymptotic behavior is concerned, the asymptotic exponential order of $\mathbb{E}_{\boldsymbol{\mu}}\left[\Pr(\mathcal{D}_1)\right]$ does not depend on the choice of γ and by following the same line of argument as above we can extend the same result for the choice of γ/M and thereof for the exponential order of $\mathbb{E}_{\boldsymbol{\mu}}\left[\Pr(\mathcal{D}_3)\right]$. As a result, we can similarly show that

$$
\mathbb{E}_{\boldsymbol{\mu}}\left[\Pr(\mathcal{D}_3)\right] \doteq \rho^{-M}. \tag{56}
$$

By noting that $\Pr(\mathcal{D}_3) \leq \Pr(\mathcal{D}_2) \leq \Pr(\mathcal{D}_1)$ and using (55) and (56) we get that

$$
\begin{aligned}
\Pr(\mathcal{D}_3) \stackrel{\cdot}{\leq} \Pr(\mathcal{D}_2) \stackrel{\cdot}{\leq} \Pr(\mathcal{D}_1) &\Rightarrow \Pr\left(\sum_{m=1}^{M} Y_m^2 < \gamma\right) \\
&= \Pr(\mathcal{D}_2) \doteq \rho^{-M}
\end{aligned}
$$

which concludes the proof.

REFERENCES

[1] E. Fishler, A. Haimovich, R. Blum, L. Cimini, D. Chizhik, and R. Valenzuela, "MIMO radar: An idea whose time has come," in *Proc. of IEEE Radar Conf.*, Philadelphia, PA, Apr. 2004, pp. 71–78.

[2] E. Fishler, A. M. Haimovich, R. Blum, L. Cimini, D. Chizhik, and R. Valenzuela, "Performance of MIMO radar systems: Advantes of angular diversity," in *Proc. 38th Asilomar Conf. Signals, Syst., Comput,*, Pacific Grove, CA, Nov. 2004.

[3] E. Fishler, A. Haimovich, and R. S. Blum, "Spatial diversity in radars—Models and detection performance," *IEEE Trans. Signal Process.*, vol. 54, no. 3, pp. 823–837, Mar. 2006.

[4] A. M. Haimovich, R. S. Blum, and L. J. Cimini, "MIMO radar with widely seperated antennas," *IEEE Signal Process. Mag.*, vol. 25, no. 1, pp. 116–129, Jan. 2008.

[5] N. H. Lehmann, A. M. Haimovich, R. S. Blum, and L. Cimini, "High resolution capabilities of MIMO radar," in *Proc. 38th Asilomar Conf. Signals, Syst., Comput,*, Pacific Grove, CA, Nov. 2006.

[6] P. Stoica, J. Li, and Y. Xie, "On Probing Signal Design for MIMO Radar," *IEEE Trans. Signal Process.*, vol. 55, no. 8, pp. 4151–4161, Aug. 2007.

[7] J. Li, P. Stoica, L. Xu, and W. Roberts, "On parameter identifiability of MIMO radar," *IEEE Signal Process. Lett.*, vol. 14, no. 12, pp. 968–971, Dec. 2007.

[8] H. Godrich, A. M. Haimovich, and R. S. Blum, "Target localization accuracy gain in MIMO radar based systems," *IEEE Trans. Inf. Theory*, 2010. [Online]. Available: http://arxiv.org/PS_cache/arxiv/pdf/0809/0809.4058v1.pdf, submitted for publication

[9] J. Li and P. Stoica, "MIMO radar with collocated antennas," *IEEE Signal Process. Mag.*, vol. 24, no. 5, pp. 106–114, Sep. 2007.

[10] I. Bekkerman and J. Tabrikian, "Target detection and localization using MIMO radars and sonars," *IEEE Trans. Signal Process.*, vol. 54, no. 10, pp. 3873–3883, 2006.

[11] B. C. Levy, *Principles of Signal Detection and Parameter Estimation*, 1st ed. New York: Springer, 2008.

[12] M. Skolnik, *Introduction to Radar Systems*, 3rd ed. New York: McGraw-Hill, 2002.

[13] S. Haykin, J. Litva, and T. J. Shepherd, *Radar Array Processing*, 1st ed. New York: Springer-Verilog, 1993.

[14] G. V. Moustakdies, "Finite Sample Size Optimality of GLR Tests," *IEEE Trans. Inf. Theory*, 2010. [Online]. Available: http://arxiv.org/PS_cache/arxiv/pdf/0903/0903.3795v2.pdf, submitted for publication

[15] M. Kendall, A. Stuart, and S. Arnold, *Advanced Theory of Statistics, Classical Inference and the Linear Model*. New York: Hodder Arnold, 1999, vol. 2A.

[16] H. V. Poor, *An Introduction to Signal Detection and Estimation*, 2nd ed. New York: Springer-Verlag, 1998.

[17] M. Balazs, "Sum of independent exponential random variables with different parameters," [Online]. Available: http://www.math.bme.hu/~balazs/sumexp.pdf

[18] M. Svecova, D. Kocur, and R. Zetik, "Object localization using round trip propagation time measurements," in *Proc. Radioelektronika, 18th Int. Conf.*, Czech Republic, Apr. 2008, pp. 1–4.

Ali Tajer (S'05) received the B.Sc. and M.Sc. degrees in electrical engineering from Sharif University of Technology, Tehran, Iran, in 2002 and 2004, respectively. He is currently working toward the Ph.D. degree in electrical engineering at Columbia University, New York.

He spent the summers of 2008 and 2009 as a Research Assistant with NEC Laboratories America, Princeton, NJ. His research interests lie in the general areas of network information theory, cognitive radios, multiuser communication, relay networks, and statistical signal processing.

Guido H. Jajamovich (S'09) received the Ingeniero Electronico degree (with honors) from the University of Buenos Aires, Buenos Aires, Argentina, in June 2006 and the M.S. degree from L'École Normale Supérieure de Cachan (ENS de Cachan), Paris, France, majoring in applied mathematics. He is currently working towards the Ph.D. degree from the Electrical Engineering Department, Columbia University, New York.

During Fall 2007, he was a visitor at the Center for Imaging Science, Applied Mathematics and Statistics Department, The Johns Hopkins University, Baltimore, MD. His research interests include statistical signal processing and genomic signal processing.

Mr. Jajamovich was recipient of the Telefonica scholarship at the University of Buenos Aires, and he earned a fellowship from the program ALFA to pursue his graduate studies in France.

Xiaodong Wang (S'98–M'98–SM'04–F'08) received the Ph.D. degree in electrical engineering from Princeton University, Princeton, NJ.

He is a Professor in the Department of Electrical Engineering, Columbia University, New York. His research interests fall in the general areas of computing, signal processing, and communications, and has published extensively in these areas. Among his publications is a book entitled *Wireless Communication Systems: Advanced Techniques for Signal Reception*, (Prentice-Hall, 2003). His current research interests include wireless communications, statistical signal processing, and genomic signal processing.

Dr. Wang received the 1999 NSF CAREER Award and the 2001 IEEE Communications Society and Information Theory Society Joint Paper Award. He has served as an Associate Editor for the IEEE TRANSACTIONS ON COMMUNICATIONS, the IEEE TRANSACTIONS ON WIRELESS COMMUNICATIONS, the IEEE TRANSACTIONS ON SIGNAL PROCESSING, and the IEEE TRANSACTIONS ON INFORMATION THEORY.

George V. Moustakides (M'82–SM'97) was born in Drama, Greece, in 1955. He received the diploma in electrical and mechanical engineering from the National Technical University of Athens, Athens, Greece, in 1979, the M.Sc. degree in systems engineering from the Moore School of Electrical Engineering, University of Pennsylvania, Philadelphia, in 1980, and the Ph.D. degree in electrical engineering and computer science from Princeton University, Princeton, NJ, in 1983.

From 1983 to 1986, he was with INRIA, France, as a Junior Researcher and from 1987 to 1990 he held a research position at the Computer Technology Institute of Patras, Patras, Greece. In 1991, he joined the Computer Engineering and Informatics department, University of Patras, as an Associate Professor, and in 1996 he became a Professor in the same department. From 2002 to 2006, he was a faculty member with the department of Computer and Communication Engineering, University of Thessaly, Volos, Greece, and in 2007 he joined the Department of Electrical and Computer Engineering, University of Patras. From 2001 to 2004, he was also a Senior Researcher (Directeur de Recherche) with INRIA, France. His interests include wireless communications, statistical signal processing, sequential detection, and signal processing for hearing aids.